Does a relation exist between the Summer North Atlantic Oscillation and sea surface temperatures?

MSc Thesis - Helga Vuist

Student number: 910201921070

Course code: MAQ-80836

Supervisors:

Prof. Dr. Wilco Hazeleger

Dr. Leo Kroon

02-08-2014

Wageningen University

Contents

Abstract V
1. Introduction 1
2. Methodology 3
2.1 Model and settings 3
2.2 Runs 3
2.2.1 Standard run 3
2.2.2 The different runs 3
3. Comparison SPEEDO output and reanalysis data 7
3.1. Overall check of the SPEEDO model 7
3.2 Global parameters 8
3.3 Spatial structure using EOF analysis 8
3.4 Correlation SNAO with standard parameters 10
4: The sensitivity of the SNAO on the SST 13
4.1 Added heat flux 13
4.2 Influence on temperature 13
4.2.1 Time series 13
4.2.2 Spatial figures 14
4.2.3 Influence on worldwide temperature 16
4.3 Influence on mixed layer depth 17
4.4 Influence on sea level pressure 18
4.5 Influence on SNAO structure 18
4.5.1 SNAO structure of hfx10 run 19
4.5.2 SNAO structure of hfx-10 run 19
4.6 Ensemble runs 20
5. Discussion 23
5.1 Comparison SPEEDO model and reanalysis data 23
5.2 The sensitivity of the SNAO on the SST 24
6. Conclusions and recommendations 27
6.1 Recommendations for further research 28
Acknowledgement 29
References 31
Appendix 1 33
Appendix 2 34

Abstract

In this study the relation between the Summer North Atlantic Oscillation (SNAO) and the sea surface temperature (SST) in the extra-tropical North Atlantic region is investigated using the SPEEDO model. It is the first time the SNAO is investigated using the SPEEDO model. A comparison between the SPEEDO output and reanalysis data shows that the model can reproduce the SNAO. The influence of the SST on the SNAO is investigated by imprinting the SST pattern belonging to the SNAO on the Atlantic Ocean. This is done by adding (extracting) an extra heat flux pattern belonging to the SNAO to (from) the regular heat flux pattern from the atmosphere to the ocean. This extra heat flux pattern is an extra compound in the system. The added extra heat flux pattern has three main areas where the extra heat flux is strong, with high positive or negative values. Due to the opposite sign, large temperature differences between the three areas developed. The changed temperature conditions caused a change in the SLP pattern: higher pressure where the temperature decreased and vice versa. Due to this changed SLP pattern the SNAO pattern is shifted. The recurrence interval did not increase. However, stronger sea level pressure anomalies can occur over Europe when the SST pattern of the SNAO is imprinted to the ocean. In the runs where the extra heat flux pattern is extracted, the SNAO weakened very much. These results imply that a relation between the SST and SNAO does exist.

1. Introduction

In the winter months the North Atlantic Oscillation (NAO) is the dominant pattern of large-scale variability in the Northern Hemisphere (Barnston and Livezey, 1987) and has been a topic of extensive research for a long time (Cornes et al., 2013; Hurrell, 1995; Robertson et al., 2000). However, the NAO is a pattern not only during the winter months, but it is a year-around pattern (Barnston and Livezey, 1987; Portis et al., 2001). The NAO in the summer months is called the Summer North Atlantic Oscillation (SNAO).

The SNAO can be defined in different ways (Folland et al., 2009), but it is often defined as the leading empirical orthogonal function (EOF) of mean sea level pressure anomaly over the extra-tropical Atlantic Ocean during July and August (Bladé et al., 2012b; Folland et al., 2009; Linderholm et al., 2012). The key figure of Folland et al. (2009) representing the SNAO is presented in Figure 1.1. The centre of the pattern is over the UK and the structure of this centre has a SW-NE direction. Over Greenland, a weak negative pole is visible.

The SNAO is weaker than the winter NAO, but it does influence weather conditions over Europe as well (Folland et al., 2009). During a positive phase, characterized by an increased pressure over northwest Europe and decreased pressure over Greenland (Bladé et al., 2012a), the weather conditions over northwest Europe are warm, dry and relatively cloud-free. Over southern Europe, the weather conditions are the opposite; cooler, wetter and cloudier (Folland et al., 2009). Although they have a similar impact on European weather, the two NAO's need to be seen differently (Feldstein, 2007).

It is interesting to understand how the NAO responds to external forcing, including sea surface temperature (SST) changes in the tropics or an increased concentration of greenhouse gases (Hurrell and Deser, 2010). According to Robertson et al. (2000) the winter NAO is correlated with SST anomalies over the (sub)tropical Atlantic Ocean. Sutton and Hodson (2003) and many others (Cassou and Terray, 2001; Sutton et al., 2000) also assume the North Atlantic SST to have impact on the winter NAO. For the winter NAO this relation has often been investigated, also with a positive result that a relation exists. Because of the differences between NAO and SNAO, it is interesting to investigate the influence of SST on the SNAO. To the author's knowledge it is the first time this relation is investigated.

The relation between the SST and SNAO will be investigated by performing a sensitivity study. We will investigate if the SNAO is sensitive to the SST in the Atlantic Region and if so, how strong is the

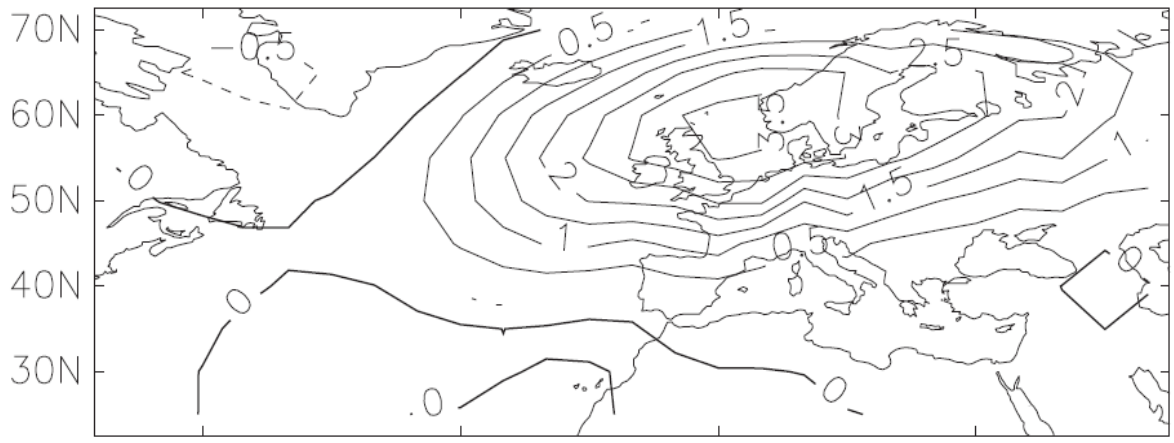

Figure 1.1: The Summer North Atlantic Oscillation (SNAO) according to Folland et al. (2009). It is constructed by taking the first covariance eigenvector of mean sea level pressure anomalies for July and August.

relation between the SST and SNAO. Next to that, a possible mechanism that can cause the relation will be explained in more depth. To perform this research, the SPEEDO (Speedy-Ocean) model (Severijns and Hazeleger, 2010) is used. The SPEEDO model is a coupled atmosphere-ocean-land model of intermediate complexity.

The main question in this report is: How does the sea surface temperature in the Atlantic region influence the Summer North Atlantic Oscillation on a seasonal time scale? To answer this question, two research questions are formulated:

- Can the SPEEDO model represent the Summer North Atlantic Oscillation and how well is this representation compared to climate observations?
- Is the Summer North Atlantic Oscillation sensitive to the sea surface temperature in the Atlantic region and what mechanism is causing the sensitivity?

The paper is structured as follows. In Chapter 2 the SPEEDO model is treated in more detail. Also the model set-up is discussed in this chapter. Chapter 3 shows if the SPEEDO model can reproduce the SNAO. In Chapter 4 the results of the sensitivity study and the possible mechanisms that can be of importance to explain the sensitivity are discussed. In Chapter 5 the discussion can be found, and the conclusions can be read in Chapter 6.

2. Methodology

2.1 Model and settings

The model used in this research is the SPEEDO model (Severijns and Hazeleger, 2010). The SPEEDO model is a coupled atmosphere-land-ocean model. It is of intermediate complexity and it is a fast model. Therefore, it is suitable for long runs. The model can resolve inter-annual variability in a recent climate setting. For these reasons the SPEEDO model is used. The model consists of a global atmosphere model (Speedy), a global ocean and sea ice model (CLIO) and a simple land-surface model. The horizontal resolution is 3.75 degrees, it has 8 vertical layers in the atmosphere and 20 vertical levels in the ocean. A number of runs have been performed with the standard settings in SPEEDO. This means that the conditions in the SPEEDO model are comparable to the 20th century climate conditions. To start the model a spin-up run of 500 years is necessary.

For different analyses in this study, a domain over the Atlantic Ocean is used. This domain is bordered by [90°W-30°E,40°N-70°N], presented in Figure 2.1. This domain is often used in many studies investigating the SNAO (Bladé et al., 2012a; Bladé et al., 2012b; Greatbatch and Rong, 2006). Taking this area, the Northern African region is not taken into account. This is due to the fact that differences between reanalysis data and real time observations are found in the Northern African region (Greatbatch and Rong, 2006). Therefore it is recommended to exclude the Northern African Region from the domain used for studies regarding the SNAO. The time period when the SNAO is present is called the high-summer months. Only July and August (JA) are taken as high-summer months. The reason for this is that according to Folland et al. (2009) the June NAO differs substantially from the NAO's of July and August.

2.2 Runs

2.2.1 Standard run

In order to compare SPEEDO data with 20th century climate observations, a standard run is performed. From the last day of the spin-up run the model is restarted. All conditions remain the same as in the spin-up run. This standard run has a duration of 100 years. The 20th century climate observations are taken from NCEP/NCAR reanalysis data (Kalnay et al., 1996). The period 1960-2000 of the reanalysis data is used for the comparison.

To compare the global SPEEDO output and reanalysis data the mean and the standard deviation are calculated for near surface air temperature, precipitation and the mean sea level pressure over the study domain. To compare the spatial patterns of SPEEDO output and the reanalysis data, an Empirical Orthogonal Function (EOF) analysis is made of the daily mean sea level pressure anomalies of the Atlantic Ocean domain for the high-summer months (JA). Correlation maps between the temperature, precipitation and mean sea level pressure and the principal component (PC) belonging to the SNAO EOF are made. These analyses are done for both the SPEEDO data and the reanalysis data.

2.2.2 The different runs

To perform a sensitivity study, different runs are performed with an adapted heat flux pattern in the Atlantic region. The runs will be discussed later, first the method of adapting the SST pattern will be discussed.

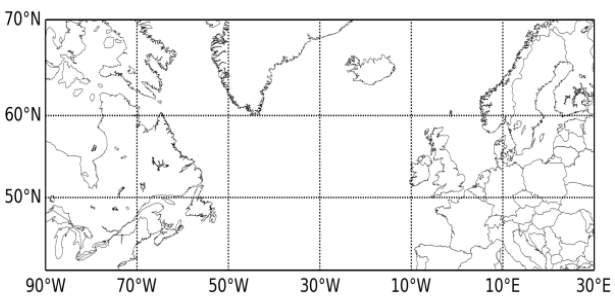

Figure 2.1: The domain that is used for the different analyses performed during this study.

The SST pattern is adapted by adding or extracting an extra heat flux pattern to or from the regular heat fluxes that are already present from the atmosphere to the ocean. This method is chosen, because extra-tropical SST anomalies are, among others, forced by surface flux anomalies (Frankignoul et al., 1998; Kushnir et al., 2002). In this study we choose explicitly to use a coupled atmosphere-ocean model and to change the SST by adapting the heat flux pattern from the atmosphere to the ocean. This is done because the heat fluxes that can occur in an only-atmosphere model with fixed SST are not realistic. By adapting the heat flux pattern, the ocean can respond to these heat fluxes, and by that it can influence the atmosphere. To investigate the relation between a specific atmospheric circulation and the SST, the SST pattern belonging to the specific atmospheric circulation can be imprinted in the ocean. This method was performed earlier by Haarsma and Hazeleger (2007).

To copy the SST pattern of the SNAO, the heat flux pattern belonging to the SNAO is computed. This is done by taking the regression between the principal component (PC) of the SNAO onto the net heat flux into the ocean. This heat flux pattern is added to the regular heat fluxes from the atmosphere to the ocean in the model. This means that the heat flux pattern is added as an extra compound to the system, it is not extracted from either the ocean or the atmosphere.

The heat flux pattern is also extracted from the regular heat fluxes from the atmosphere to the ocean. Again, the heat flux pattern that is extracted is removed from the system, it does not stay in the atmosphere. The heat flux pattern is extracted from the regular heat fluxes, to investigate how the atmosphere and the SNAO will react on an ocean which is less favourable for developing a SNAO, because the SST pattern of the SNAO is removed from the ocean.

To investigate the sensitivity of the SST onto the SNAO, two different set-up for the runs are performed. A number of 100-year runs where the extra heat flux pattern is added or extracted are performed. During these runs, the extra heat flux is constantly added to or extracted from the regular heat fluxes. This causes a constant SST pattern belonging to the SNAO. To get a clear signal, the added or extracted heat fluxes are multiplied by 1, 2, 5 or 10. This means that in total 8 different 100-year runs are performed, four runs with the added heat flux pattern multiplied by 1,2,5 or 10 and also four runs with the extracted heat flux pattern multiplied by 1,2,5 or 10.

Next to that, two 100-member ensemble runs are executed. One ensemble run with the added heat flux pattern multiplied by 10 and one ensemble run with the extracted heat flux pattern multiplied by 10. The duration of one member of the ensemble is one year. The start dates of the ensemble member runs are every first of January of the standard run. Then, the model runs normally for 3 months. During April, May and June the heat flux pattern multiplied by 10 is added or extracted. From July the model is running normally again. The ensemble run is performed to investigate the inter-annual variability of the SNAO. The runs that are discussed in the results and the discussion are the 100-year runs, unless when it is mentioned differently.

A summary of all runs that are performed in this study is present in Figure 2.2. The runs where the heat flux pattern is added to the regular heat fluxes get the index hfx 'number of multiplies'. The runs where the heat flux is extracted get the index hfx- 'number of multiplies'. For example, the run where the heat flux multiplied by 10 is added to the regular heat fluxes receives the name 'hfx10'.

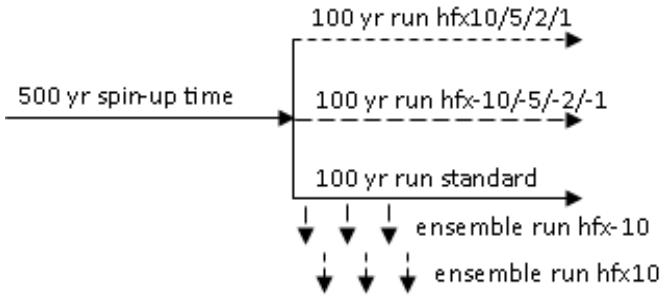

Figure 2.2: The runs that are performed during this study. In the text a more detailed explanation is given about the different runs.

With these two different set-up for the runs, the sensitivity of the SNAO is investigated. This is done by performing the EOF analysis for the different runs and compare them to the standard run. Also a histogram of the SLP anomalies in the domain of [7.5°W-30°E,40°N-70°N] is calculated for both run set-ups. With these tools we will study if and how the SNAO pattern is changed.

3. Comparison SPEEDO output and reanalysis data

To investigate the SNAO using the SPEEDO model, the first step is to check if the SPEEDO model can reproduce the SNAO. This is necessary, because to the author's knowledge it is the first time the SNAO is investigated using the SPEEDO model. We compare the SNAO output with NCEP/NCAR reanalysis data (Kalnay et al., 1996). This comparison is performed in three steps. In Section 3.2, some standard parameters are calculated for both data sets and compared. Secondly, the spatial structure of the SNAO is compared using Empirical Orthogonal Function (EOF) analysis (Section 3.3). Finally, the influence of SNAO on the precipitation and temperature over Europe is compared using correlation maps (Section 3.4).

3.1. Overall check of the SPEEDO model

Before the SPEEDO output can be compared to reanalysis data, it is important to check if the SPEEDO model runs properly. To do this, the global 2 meter temperature (T_{2m}) is calculated and compared with the T_{2m} found by Severijns and Hazeleger (2010). In their paper they found a global T_{2m} of 285.3 K. The global T_{2m} that is found in this study is 285.4 K. Also other variables, such as the zonal wind at 925 hPa and the global stream function, are compared (not shown). The figures are almost similar. This means the model runs properly.

Table 3.1: The global mean values and the standard deviation of the sea level pressure (SLP), precipitation (Prec) and the near surface air temperature (T_0) for 100 year of SPEEDO output and 40 year (1960-2000) of reanalysis data.

Quantity	SPEEDO model		Reanalysis data	
	Mean	St. dev.	Mean	St. dev.
SLP (hPa)	1011.64	0.45	1012.93	0.53
Prec (mm/day)	2.73	0.98	2.28	0.24
T0 (K)	287.77	1.20	288.08	1.09

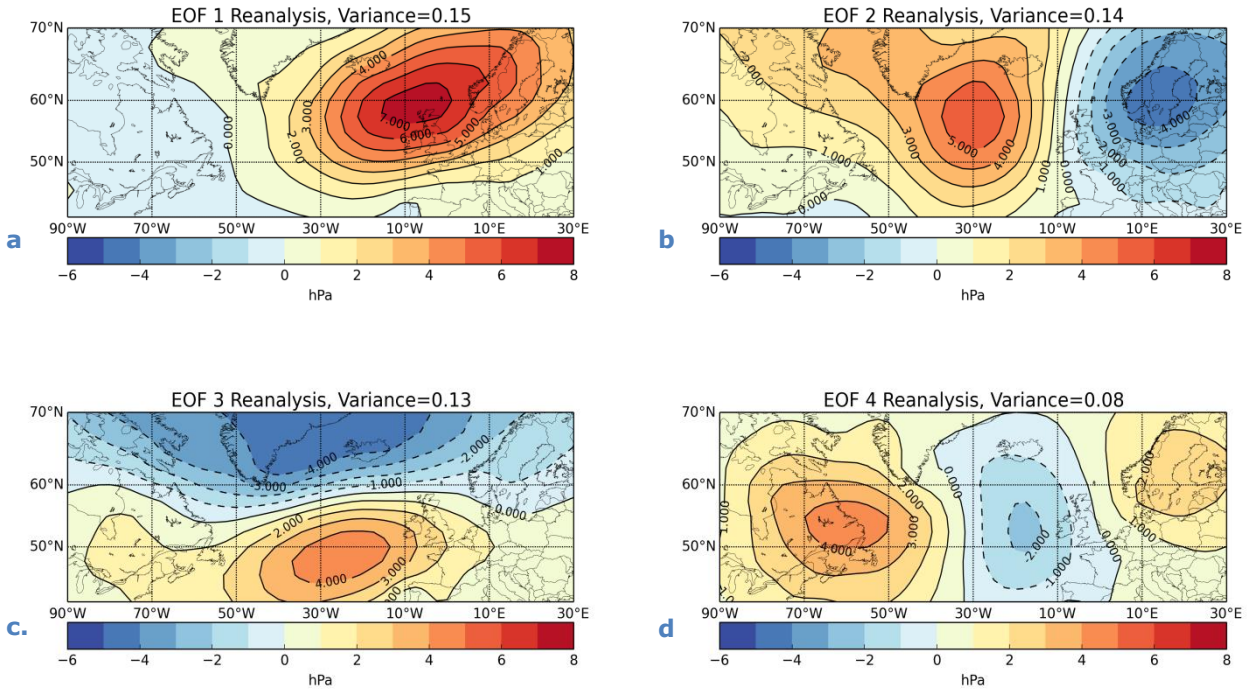

Figure 3.1: The main four EOF modes of the reanalysis data. The EOFs are calculated by taking the covariance eigenvector of daily high summer (JA) SLP anomalies over the region [90°W-30°E,40°N-70°N] over a time period of 40 years (1960-2000).

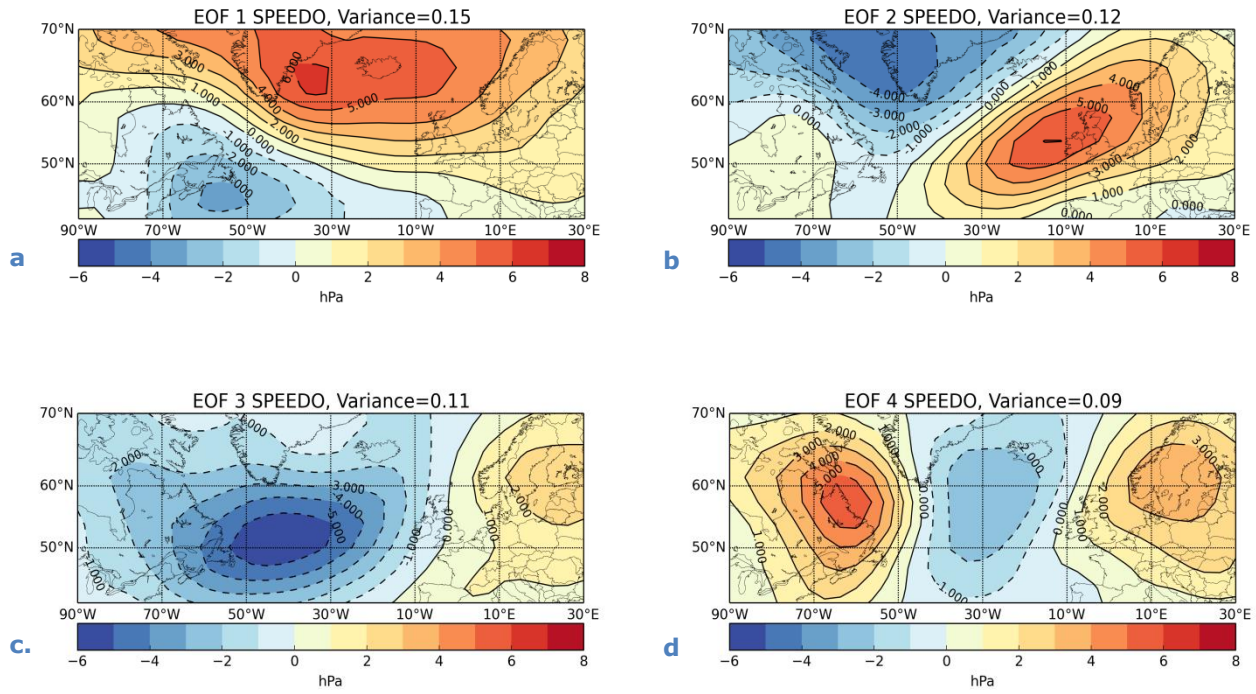

Figure 3.2: The main four EOF modes of the SPEEDO output. The EOFs are calculated by taking the covariance eigenvector of daily high summer (JA) SLP anomalies over the region [90°W-30°E,40°N-70°N] over a time period of 100 years.

3.2 Global parameters

To compare the SPEEDO model with the reanalysis data, some standard statistical parameters are calculated for both data sets. The mean and standard deviation of the global sea level pressure (slp), precipitation (prec) and near surface air temperature (T_0) are calculated. The results are summarized in Table 3.1. The SLP mean of SPEEDO output and reanalysis data differ by 0.12%. This is just a small difference. The difference of T_0 is even smaller, 0.10%. Both parameters are well represented by the SPEEDO model. The global precipitation is overestimated by the SPEEDO model by 16.4%.

The standard deviation of the SLP and T_0 of both data sets is in the same order of magnitude. The standard deviation of the precipitation is also too large compared to the reanalysis data. However, the overestimation of the precipitation will not lead to serious problems, because precipitation is not of importance for determining the SNAO. The other parameters are well represented by the SPEEDO model, so the model can be used.

3.3 Spatial structure using EOF analysis

The SNAO is defined as the leading Empirical Orthogonal Function (EOF) of daily mean sea level pressure (SLP) anomalies over the extra-tropical Atlantic Ocean in July and August (Bladé et al., 2012b; Folland et al., 2009). The extra-tropical Atlantic Ocean area is defined in this study by [90°W-30°E, 40°N-70°N]. EOF modes show the dominant pattern over a specific area and time. The variance of a EOF mode indicates how often this pattern is present. The main 4 EOF modes of reanalysis data are presented in Figure 3.1. In Figure 3.2 the main 4 EOF modes of the SPEEDO output are presented.

In Figure 3.1 the SNAO is clearly visible as the first EOF mode, and it explains 15% of the variance. It is a monopole, situated to the north of the United Kingdom with a southwest-northeast orientation. The second EOF mode is a west-east dipole, while the third EOF mode is a north-south dipole. The fourth EOF mode is a tripole, this last pattern explains only 8% of the variance.

The SPEEDO output gives a slightly different set of patterns. The first EOF mode also explains 15% of the variance. However, the pattern is a north-south dipole, comparable to the third EOF mode of the reanalysis data. The second EOF mode is a dipole where the poles have a SW-NE orientation. The strongest pole of this dipole is situated just west of the United Kingdom. Due to the SW-NE orientation the positive pole looks like the first EOF mode of the reanalysis data. The negative pole of this dipole is situated over the west of Greenland. The third EOF mode is a west-east dipole and the forth EOF mode is a tripole. The fourth EOF mode of SPEEDO is comparable to the fourth EOF mode of the reanalysis data. When comparing the third EOF mode of SPEEDO and the second EOF mode of the reanalysis (they are both a west-east dipole), the west dipole of SPEEDO is situated a bit more to the south-west and it has a different form. However, the differences of this EOF mode are beyond the scope of this research.

Interesting for this research is the difference between the first EOF mode of reanalysis and the second EOF mode of SPEEDO , because these EOF modes are assumed to be representing the SNAO. Bladé et al. (2012a) investigated the SNAO in CMIP3 models. For determining the SNAO in the different runs they used the following principle: the SNAO is characterized by a SLP dipole with the structure of the pole in a SW/NE orientation. They found that the location of the southern pole is variable. In some runs the position of it is even in the centre of the Atlantic. Also in different runs the SNAO is represented by the second EOF mode. In the SPEEDO output the SNAO is also represented as a dipole and as the second EOF mode. The first EOF of reanalysis data is comparable to the first EOF Folland et al. (2009) found (their figure 1a). The EOF by Folland et al. (2009) is made using the daily MSLP analysis by Ansell et al. (2006). Both EOFs are a monopole and they are present at the same location.

In the SPEEDO data the SNAO is represented by the second EOF mode. The variances of the main four EOF modes are in a small range (15% to 9%), and because of that the patterns cannot be distinguished and therefor they can be switched easily between the different EOF modes. However, the variance that is explaining the EOF1 of the reanalysis data and EOF2 of the SPEEDO data are of the same order of magnitude 15% against 12%. It is also comparable to the results of Folland et al.

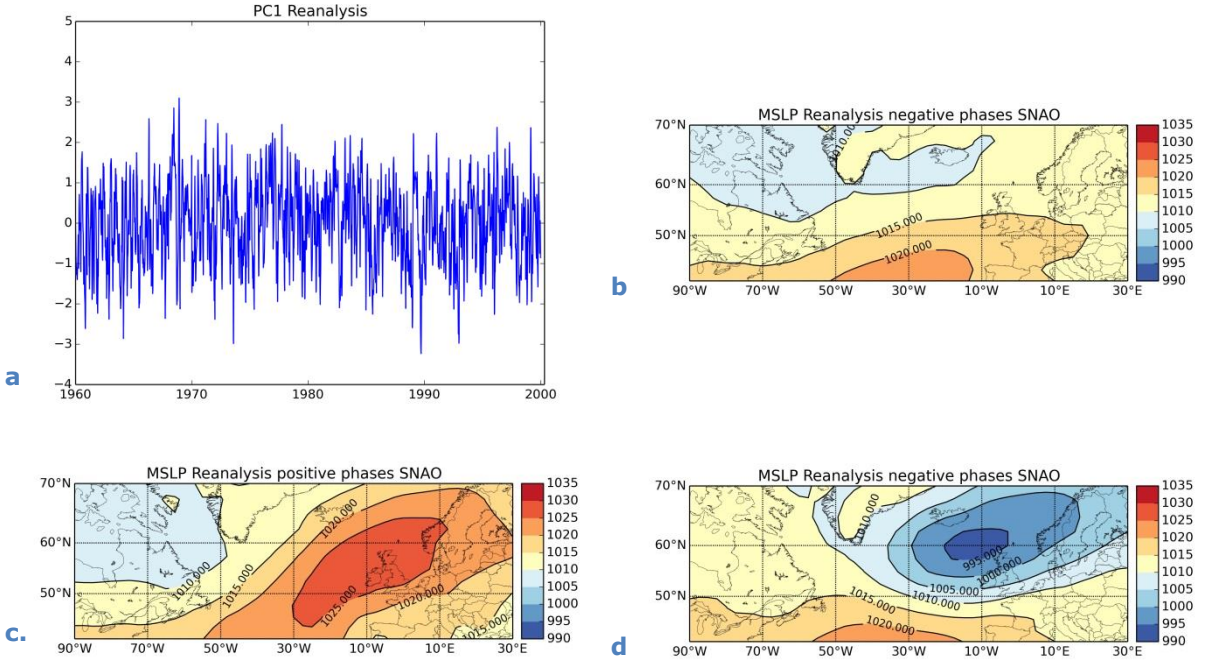

Figure 3.3: a) The principal component (PC) of the reanalysis data. b) The JA average MSLP pattern in the Atlantic region. c) The MSLP pattern during strongly positive phases of the SNAO. d) The MSLP pattern during strongly negative phases of the SNAO.

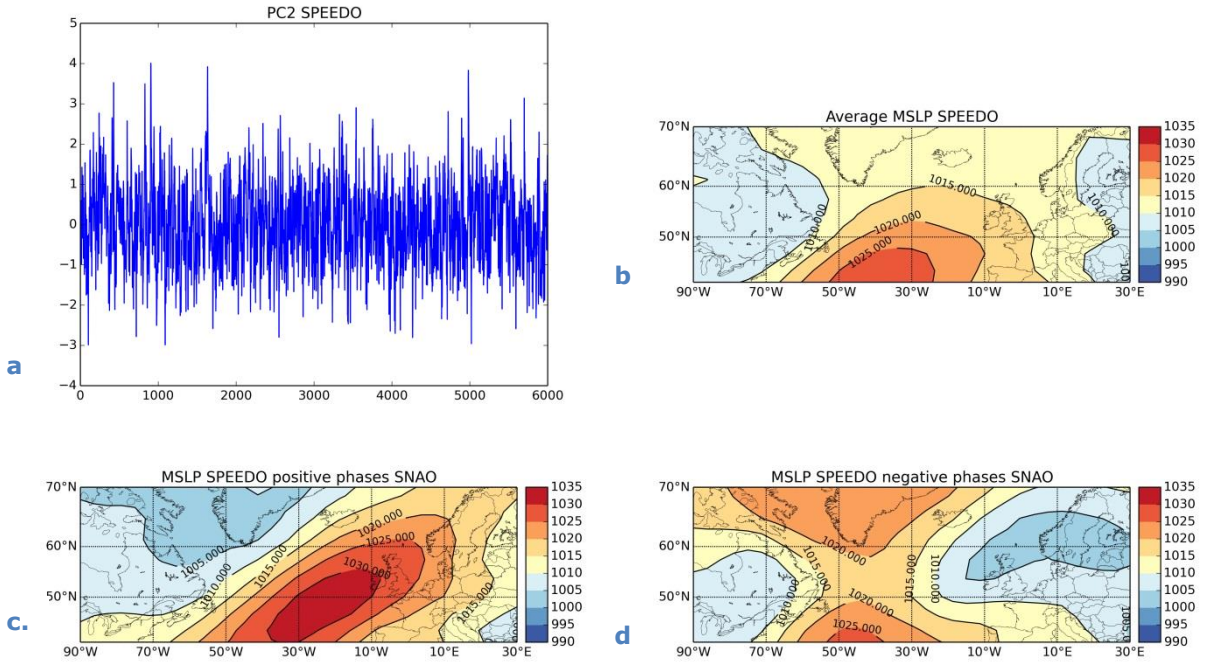

Figure 3.4: Same as Figure 3.3, but for the SPEEDO output.

(2009). They found that the EOF representing the SNAO explains 18% of the variance. This is approximatly equal to the value of the reanalysis data (15%) and the SPEEDO output (12%) .

Another way to compare the spatial pattern of the SNAO is to take from both the reanalysis data and the SPEEDO output a couple of strongly positive SNAO patterns and a couple of strongly negative SNAO phases. These positive and negative phases can be taken from the principal component, and they are defined as strongly positive or strongly negative if the PC value is respectively above 2 or below -2. The principal component (PC) is a time series belonging to an EOF mode. Figure 3.3 presents the PC of the reanalysis data, the JA average mean sea level pressure (MSLP) pattern and the MSLP pattern during strongly positive and strongly negative phases. In Figure 3.4 the same figures are presented for the SPEEDO output.

From these figures it appears that the JA average MSLP pattern of the SPEEDO output and reanalysis data are slightly different in strength. However, the location and the shape of the high pressure system are the same. The spatial patterns of the strongly positive SNAO patterns of the reanalysis data and the SPEEDO output are comparable. However, as already seen in the EOF analysis, the negative pole over Greenland is weaker for the reanalysis data. For the negative SNAO phase, the low pressure centre above the UK for the reanalysis data is lower than the low pressure centre of the SPEEDO output. However, in both the reanalysis data and the spatial pattern are comparable.

3.4 Correlation SNAO with standard parameters

The SNAO influences the temperature and precipitation in Europe. This influence is mostly in the north-western part of Europe, but the weather in the Mediterranean region is also influenced by the SNAO (Bladé et al., 2012b). A correlation analysis is performed to compare the influence of the SNAO on the temperature and precipitation for SPEEDO output and reanalysis data. This is done by constructing correlation maps. The correlation between the variable (T_0 or Prec) and the principal component (PC) of the SNAO is calculated for every grid point in the domain [90°W-30°E, 40°N-70°N]. The first PC (PC1) of reanalysis is correlated with the precipitation and temperature of the reanalysis data. To calculate the correlation maps for the SPEEDO output, the second PC (PC2) is used. This is done because the second EOF is representing the SNAO.

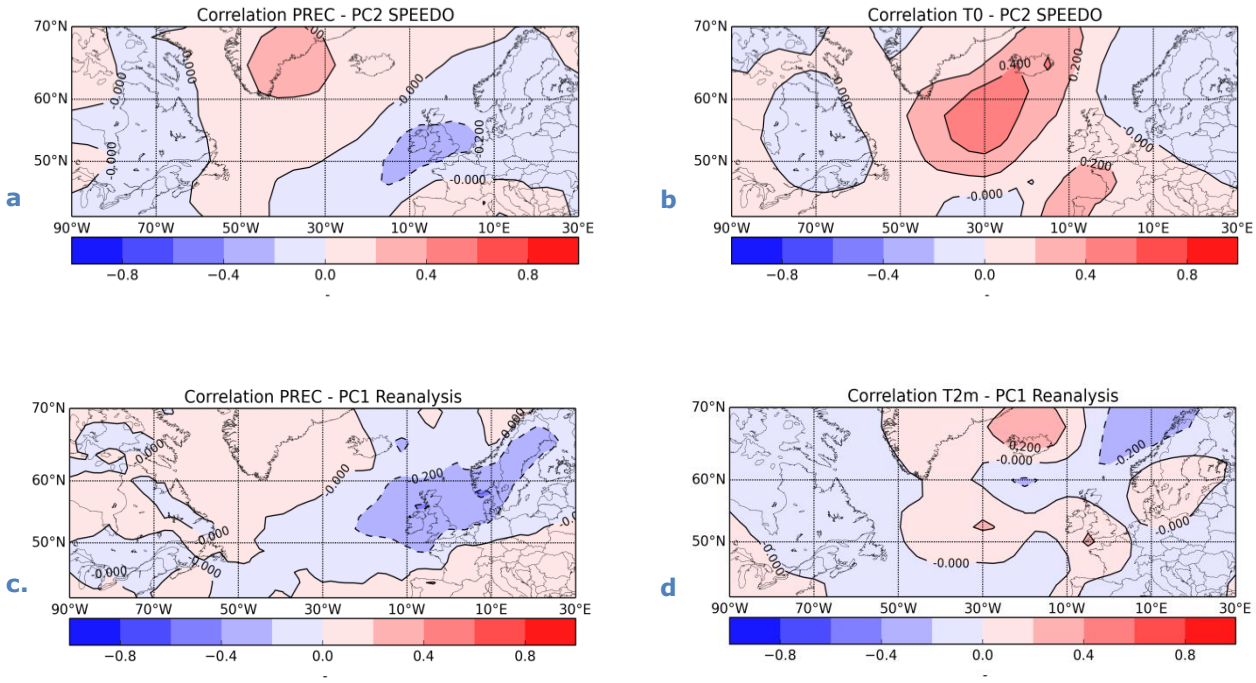

Figure 3.5: Correlation maps between the precipitation (PREC) or near surface air temperature (T_0) and the principal component (PC). For reanalysis data the first PC (PC1) is used. The second principal component (PC2) of the SPEEDO output is used.

In Figure 3.5 the correlation maps of the SPEEDO output and the reanalysis data are presented. In the correlation maps of the precipitation (Figure 3.5a and Figure 3.5c) a negative correlation over the NW of Europe is present. This means that when the SNAO is strong, less precipitation will occur over this part of Europe. The reanalysis data does not show a significant correlation elsewhere in the domain, while the SPEEDO output shows a positive correlation between the SNAO and precipitation over Greenland. Nevertheless, the correlation maps are comparable.

The correlation maps of T_0 of SPEEDO output and reanalysis data show large differences. According to the reanalysis data, almost no correlation exists over Europe, while SPEEDO output gives a correlation of 0.2 over SW-Europe. The reanalysis data has a negative correlation between the SNAO and temperature to the west of Norway, while the SPEEDO output gives no negative correlations for the temperature in this region. The correlation over Iceland is present in both datasets. However, this correlation is much stronger in the SPEEDO output than in the reanalysis data. How these differences between the correlation maps of the SPEEDO output and the reanalysis data can be explained can be read in Chapter 5.

To summarize this chapter it can be said that the SPEEDO model can reproduce the SNAO. However, the SNAO is resembled by the second EOF mode in the SPEEDO model, compared to the first EOF mode of the reanalysis data. This is due to the fact that the explained variances of the different EOF modes are in a small range. The mean sea level pressure pattern of strongly positive and negative SNAO phases and to less extend the correlation between the principal component and the near surface air temperature or pressure are very comparable between the SPEEDO output and reanalysis data.

4: The sensitivity of the SNAO on the SST

The main question of this study is if the SNAO is related to the sea surface temperature in the Atlantic Ocean. To answer this question, the sensitivity of the SNAO on the SST is investigated. The results of this sensitivity study are presented in this chapter. First, the added heat flux is discussed and the response of that on the near surface air temperature. After that the influence on the sea level pressure is discussed. Last the main result will be presented, namely if the structure of the SNAO is changed. First, the focus is on the 100-year runs, in section 4.6 the results of the ensemble runs will be discussed.

4.1 Added heat flux

To adapt the sea surface temperatures, a heat flux pattern is added to or extracted from the ocean. In Chapter 2 this principle is explained in more detail. The heat flux pattern that is added or extracted to or from the regular heat fluxes from the atmosphere to the ocean is given in Figure 4.1a. The heat flux pattern consists of three areas where the flux is very high. One large area in the middle of the Atlantic Ocean, one to the west of Norway and one around 40°N, 30°W. However, the heat flux in the areas to the west of Norway and in the south have an opposite sign than the heat flux in the mid-Atlantic Ocean. So when the heat flux pattern of Figure 4.1a is added to the regular heat fluxes, an extra heat flux is added in the mid-Atlantic, but less heat will reach the ocean to the west of Norway and around 40°N, 30°W, compared to the standard run. When the heat flux pattern is extracted from the regular heat fluxes, the extra heat flux in the areas to the west of Norway and around 40°N, 30°W is added to the regular heat flux from the atmosphere to the ocean and less heat will reach the ocean in the mid-Atlantic Ocean. For the sake of completeness, this pattern is presented in Figure 4.1b.

4.2 Influence on temperature

4.2.1 Time series

The effect of the added or extracted heat flux pattern on the near surface air temperature is investigated by constructing time series of the 100-year runs. The time series are presented in Figure 4.2. The time series of JA averaged near surface air temperatures are constructed over two different areas, over [50°W-10°W, 50°N-70°N] and [10°W-30°E, 50°N-70°N]. These areas are chosen because in these areas the added heat flux is strong, but with opposite signs. The areas are indicated by the black boxes in Figure 4.1a. In the domain of [10°W-30°E] the extra heat flux is negative for the runs where the heat flux is added to the regular heat fluxes. This means that less energy will reach the ocean than in the standard run. For the runs where the extra heat flux is extracted from the regular heat fluxes more energy will reach the ocean. In the [50°W-10°W] domain this is the opposite, more energy for the added run and less energy for the extracted run.

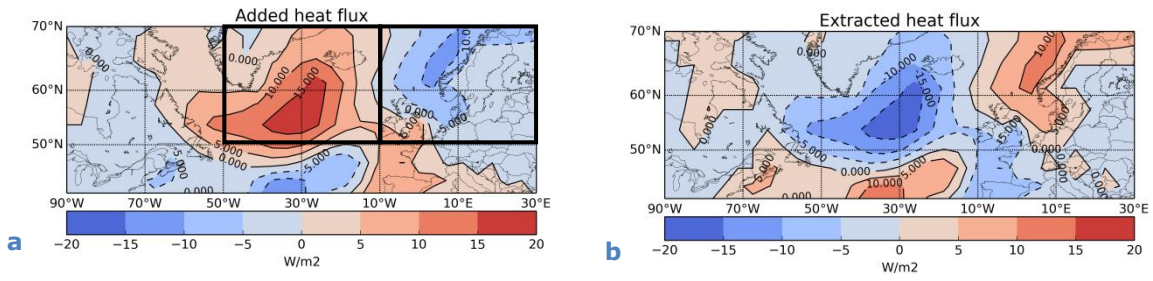

Figure 4.1: a. The heat flux that is added or extracted to the regular heat fluxes from the atmosphere to the ocean. b. The pattern of the extra heat flux when the flux is extracted from the regular het fluxes. The black boxes indicate the areas where JA averaged time series of the temperature are constructed.

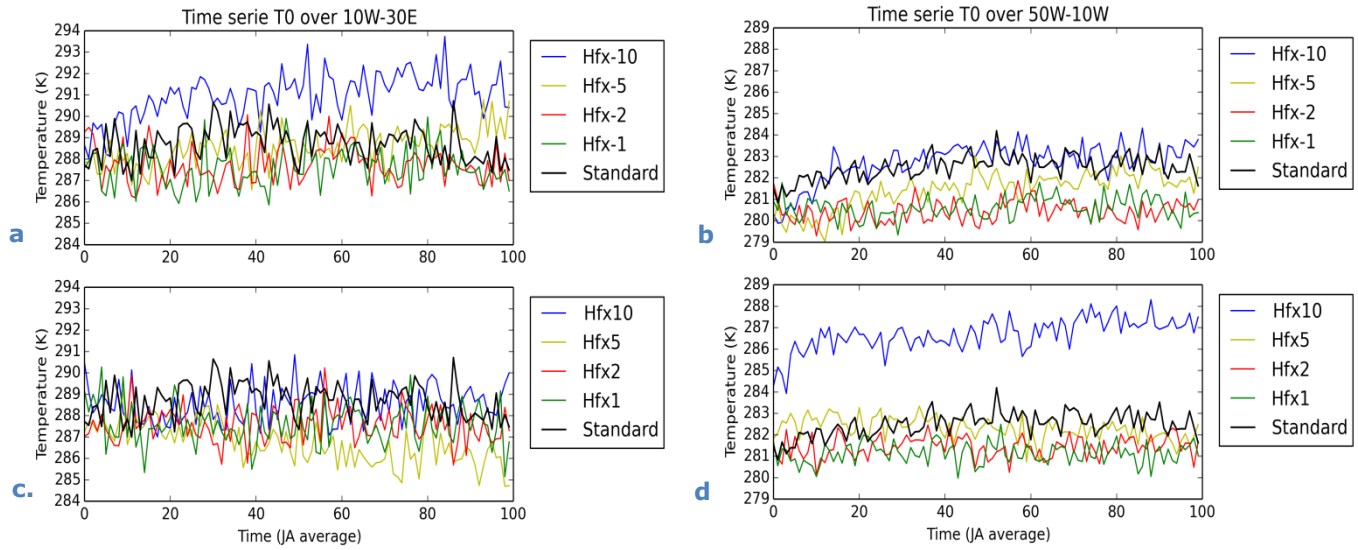

Figure 4.2:. A. The T0 time series of the [10°W-30°E, 50°N-70°N] domain for the runs where the extra heat flux is extracted from the regular heat fluxes. B. Same domain as Figure 4.2a, but for the runs where the extra heat flux is added to the regular heat fluxes. C. Same was Figure 4.2a, but for the domain of [50°W-10°W, 50°N-70°N]. d. Same as Figure 4.2b, but for the domain of [50°W-10°W, 50°N-70°N].

In Figure 4.2a the difference of the near surface air temperature between the hfx-10 run and the other runs is clearly visible. The temperature in this area is 3-5 K higher than the other runs. This can be explained by the added heat flux in this area for the hfx-10 run [10°W-30°E]. Per day up to 100 W/m^2 is added in this area, probably causing high near surface air temperatures. For the hfx10 run (Figure 4.2c) up to 100 W/m^2 is extracted from the ocean in this area. However, this effect is not visible in the near surface air temperature. The temperature of the hfx10 is in the same order as the standard run and the other runs (hfx5/2/1).

In the other domain, [50°W-10°W], the effect of the added heat flux is clearly visible in the hfx10 run (Figure 4.2d). In this area the heat flux is added to the ocean with even a value up to 150 W/m^2. This causes a difference of 5-7 K. The effect of the extracted heat flux in the hfx-10 run is not present (Figure 4.2b), although the extracted heat flux is also up to 150 W/m^2.

The temperature response of the heat flux is the same in both domains. A strong response is present where the heat flux is added to the ocean and a weak to no response is present where the heat flux is extracted from the ocean.

A clear result of these time series is that only a clear response is visible in the hfx10 and hfx-10 runs and not for the hfx5/-5, hfx2/-2 and hfx1/-1 runs. For that reason, in the rest of the paper only the hfx10 and hfx-10 runs will be discussed.

4.2.2 Spatial patterns

In the time series it is visible that the near surface air temperature responds differently to added or extracted heat flux patterns. This difference is also visible when spatial figures of the temperature are created. For every grid cell the difference between the JA average temperature of the hfx10/hfx-10 run and the standard run is calculated. These figures are presented in Figure 4.3a (hfx10 run) and Figure 4.3b (hfx-10 run).

Over the mid-Atlantic Ocean the average JA temperature of the hfx10 runs is more than 6 K higher than the standard run. To the west of Norway the JA average temperature is around 1.5 K lower than the standard run. However, in this area the heat that is extracted is up to 100 W/m^2. For the hfx-10

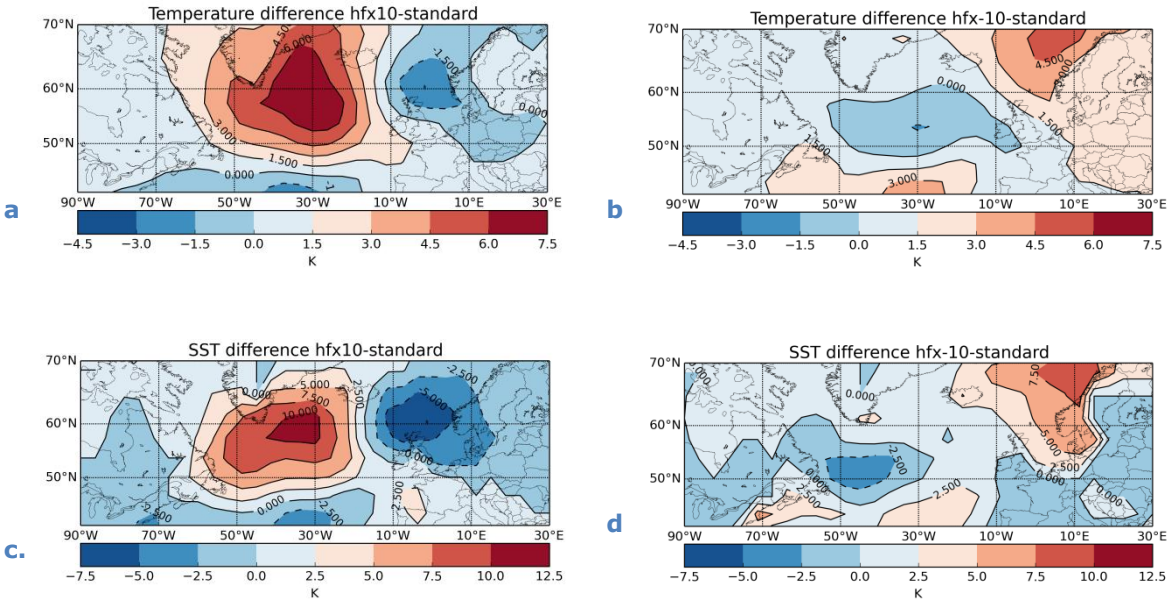

Figure 4.3: Temperature differences (a-b) and SST differences (c-d). Calculated by taking the average JA temperature over 100 year of the hfx10 (a/c) or hfx-10 (b/d) minus the average JA temperature over 100 year of the standard run.

run the temperature to the west of Norway is around 4.5 K higher than the standard run. The temperature decrease over the mid-Atlantic Ocean is almost not visible. Over a really small area the temperature decreased by 1.5 K, over the rest of the Atlantic Ocean the decrease is even less than 1.5 K. So the non-linearity that is visible in the time series can also be found in the spatial figures of the temperature differences.

For all analyses the near surface air temperature is taken instead of the SST. This is done because the near surface air temperature is strongly comparable to the underlying SST (Wallace and Hobbs, 2006). For the sake of completeness, the spatial pattern of the SST difference between the average 100 year temperature of the hfx10 and hfx-10 runs and the standard run for every grid point is also presented in Figure 4.3. The areas with the high near surface air temperature differences are well situated compared to the spatial pattern of the SST differences.

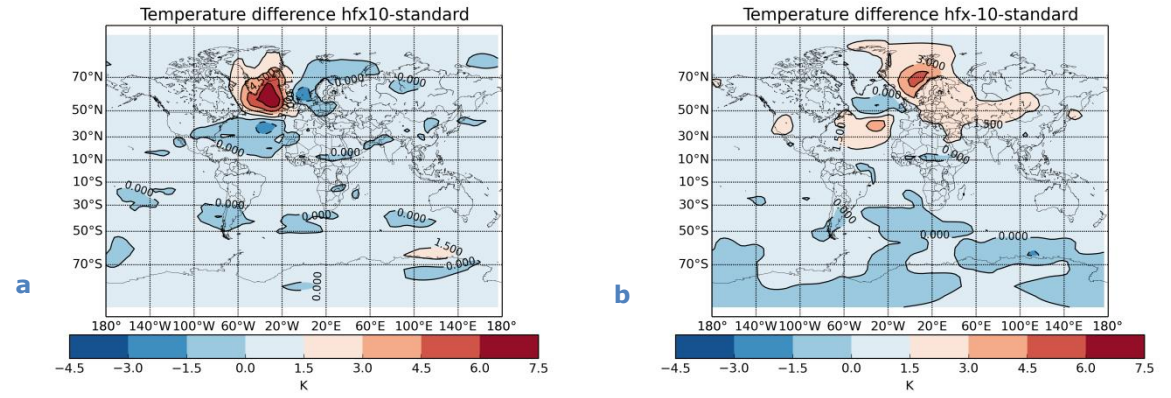

Figure 4.4: Same as Figure 4.3a and Figure 4.3b, but for the whole world.

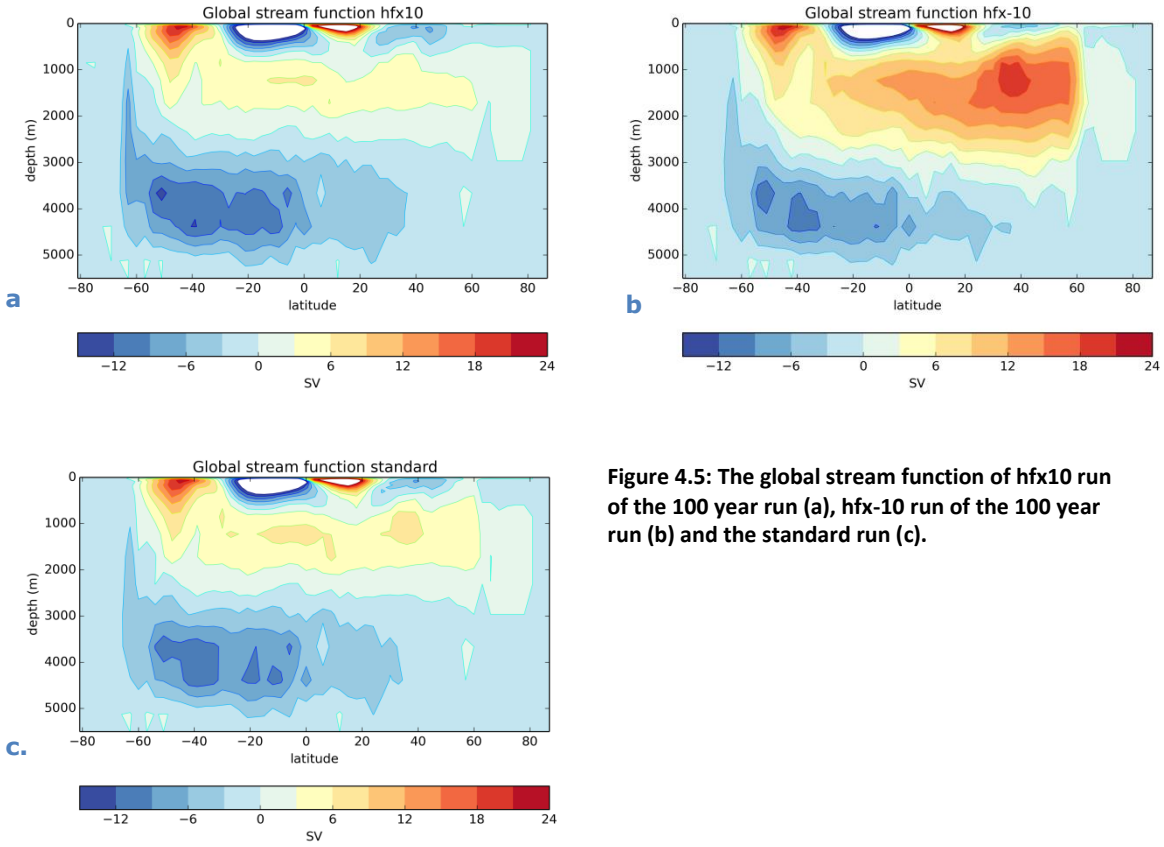

Figure 4.5: The global stream function of hfx10 run of the 100 year run (a), hfx-10 run of the 100 year run (b) and the standard run (c).

4.2.3 Influence on worldwide temperature

When the temperature difference between the hfx10 and hfx-10 of the 100-year runs and the standard run was calculated, something remarkable showed up at the edge of Antarctica. The near surface air temperature changed also a lot around 65°S, 120°E. Because of that, this section is added to this study.

In Figure 4.4 the temperature differences between the hfx10 and hfx-10 runs of the 100-year runs and the standard run are presented for the whole world. It appears that the temperature responds on the added or subtracted heat flux around 65°S, 120°E. In the hfx10 run (Figure 4.4a) the temperature on this location increased by 1.5 K. For the hfx-10 run, the temperature decreased by 1.5 K (Figure 4.4b). However, the response of the hfx-10 run is slightly less than the hfx10 run. These differences implies that the overall ocean circulation has been changed due to adding or extracting heat fluxes in the Atlantic region.

The overall sea circulation can be investigated using the global stream function. The global stream functions of the hfx10 and hfx-10 runs and the standard run are presented in Figure 4.5. In the stream function, four main cells are visible. Two cells are visible near the equator, with a depth of 500 meters. These cells are called ventilated thermoclines (VT). The cell in the mid ocean is called the North Atlantic Deep Water (NADW), and it is reaches till a depth of 3000 meters. The bottom cell is called the Antarctic Bottom Water (AABW) and is situated very deep, between 3000 and 5000 meters (Vallis, 2006).

According to Hartmann (1994) two mechanisms have a large influence on the flow in the ocean, namely wind-driven and density-driven components. The VT cells near the equator are wind-driven and the NADW and AABW cells are density driven. The density driven cells have a larger influence on the global circulation (Hartmann, 1994). Next to that, the wind driven cells are situated at the

equator, where nothing has changed during the sensitivity study. Due to this, only the NADW and AABW cells are investigated in more depth.

The formation of these two cells is slightly different. The NADW develops because warm, saline water flows from the equator pole ward. Near the poles, the water is exposed to very cold temperatures, and due to the cooling the water becomes dense enough to sink. Also the water in the Southern Oceans can be dense enough to sink to great depths (Hartmann, 1994). This sinks even deeper than the NADW.

In the hfx-10 run, more heat flux is extracted from the ocean in the Atlantic region, causing a colder upper ocean. Due to the colder ocean in this area, the water becomes denser and it sinks faster. This happens around 60°N. This is visible in Figure 5.7b. Due to this, the NADW circulation becomes stronger and more water is transported to the south. Due to that, more water reaches the surface around 65°S. This water is cooler than the water that reaches the surface in the standard run. This can explain the negative temperature difference of the hfx-10 run.

For the hfx10 run the process is the opposite. More heat is added, causing higher ocean temperatures, so the water becomes less easily dense around 60°N. Due to this, the NADW circulation slows down. When the NADW circulation becomes less, the AABW circulation can become stronger, causing higher temperature reaching the surface at 65°S than the standard run. This caused the positive temperature difference at 65°S,120°E.

4.3 Influence on mixed layer depth

The different response of the near surface air temperature on the added or extracted heat fluxes might be connected to a different response of the ocean to the added or extracted energy, because according to e.g. Spall et al. (2000) and Hartmann (1994) a balance between local surface heat fluxes and vertical mixing in the ocean exists. The depth of a mixed layer depends on the generation of buoyancy in the ocean. When the surface is strongly cooled, e.g. by surface heat fluxes, dense water is formed near the surface and it will sink within the mixed layer. Warmer water is transported upward, and this is causing more buoyancy. Due to this process, the mixed layer is growing. When the surface is heated, the generation of mixing by buoyancy is less and the mixed layer will become thinner and warmer (Hartmann, 1994).

To investigate if this is the reason for the different responses of the temperature, the difference in the average depth of the mixed layer is calculated. It is calculated by taking the difference between the JA average mixed layer depth of the hfx10 run or the hfx-10 run and the JA average of the standard run. Again, this is calculated for the 100-year run. The results of the differences in mixed layer depth are presented in Figure 4.6.

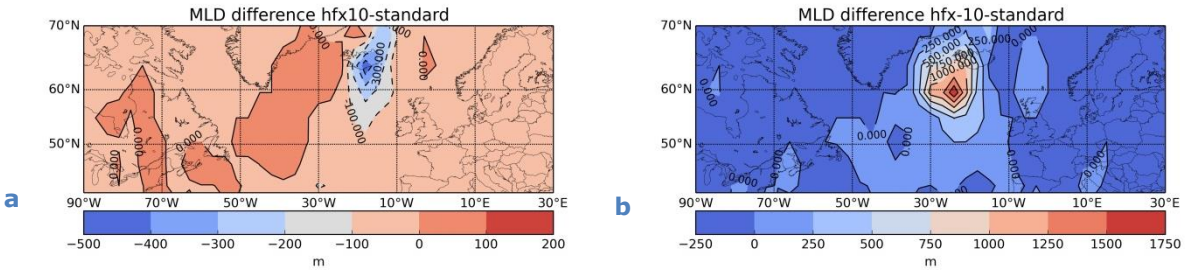

Figure 4.6: The JA averaged mixed layer depth difference between the hfx10 (a) or the hfx-10 (b) run and the standard run.

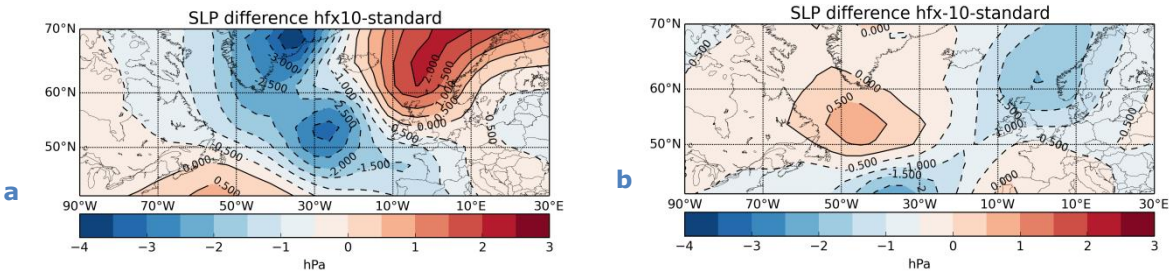

Figure 4.7: The JA average SLP difference between the hfx10 (a) or the hfx-10 (b) and the standard run.

Figure 4.6 shows that the mixed layer depth of the ocean has changed. In the hfx10 run heat is added to the ocean, and the mixed layer became shallower. The difference between the JA averaged mixed layer depth of the hfx10 and the standard run is negative, implying that the mixed layer depth of the hfx10 is smaller. The area where the mixed layer depth became shallower is situated a little bit to the north east of the large area where the large temperature difference is visible. In Figure 4.6b it is visible that the difference of the mixed layer depth is even larger between the hfx-10 run and the standard run. The mixed layer depth of the hfx-10 run became 1750 meters deeper than the standard run.

4.4 Influence on sea level pressure

Due to the changed heat fluxes, the near surface air temperature and the mixed layer depth of the ocean are changed. However, the main question is if the pattern of the SNAO is changed. To investigate this, it is important to know how the sea level pressure pattern is changed in the area. This is due to fact that the SNAO pattern is a specific sea level pressure pattern. The difference between the sea level pressure of the hfx10/hfx-10 run and the standard run is calculated and presented in Figure 4.7. Again, the difference between the JA average sea level pressure of the hfx10/hfx-10 run and the standard run is calculated for every grid cell. In Figure 4.7a it is visible that the sea level pressure increased over the area to the west of Norway in the hfx10 run. At the same time, the sea level pressure decreased over the Mid-Atlantic region and also over Greenland. An increase or decrease of the sea level pressure in the hfx-10 is much less clear. To the west of Norway, the sea level pressure decreased by around 1.5 hPa. Also a decrease is visible in the area of 40°N,30°W. Over the western part of the North Atlantic ocean and over SW-Europe a small increase in SLP is visible. These results imply that the sea level pressure pattern is changed.

4.5 Influence on SNAO structure

The sea level pressure pattern has changed due to the added or extracted heat flux pattern. As said before, the SNAO pattern is a specific sea level pressure pattern. A change in the SNAO pattern can be seen by comparing the EOF of the hfx10 and hfx-10 run with the standard run. In section 4.5.1 the

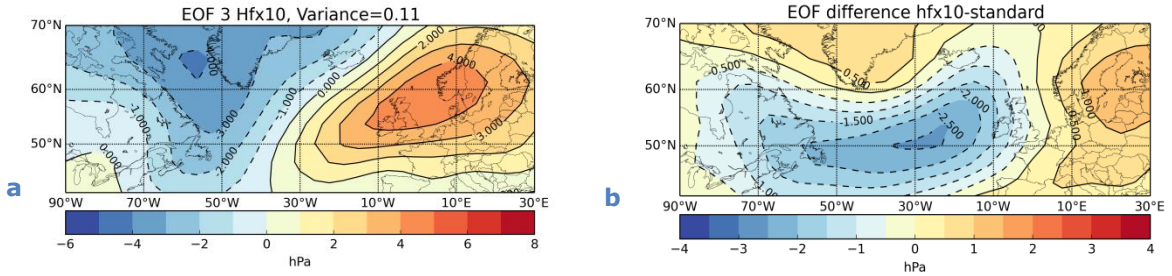

Figure 4.8 : a) The EOF that resembles the SNAO for the hfx10 run. b) The difference between EOF3 hfx10 and EOF2 standard.

influence of the heat fluxes on the SNAO of the hfx10 run is discussed. In section 4.5.2 the spatial pattern of the SNAO of the hfx-10 run is discussed.

4.5.1 SNAO structure of hfx10 run

In Figure 4.8a the EOF mode belonging to the SNAO of the hfx10 run is presented. The other EOF modes of the hfx10 run are added to this report in Appendix 1. A remarkable difference between the standard SNAO EOF mode (Figure 3.2b) and the SNAO EOF of the hfx10 is that SNAO in the hfx10 run is represented by the third EOF mode, compared to the second EOF mode of the standard SNAO. This is due to the fact that the explained variance is 1% lower for the hfx10 run. Like the explained variances of the standard EOF modes, the variance between the first and the fourth EOF mode of the hfx10 runs is 7-8%. Because the spread in variability is so small, the EOF mode that is explaining the SNAO can be changed very quickly. Nevertheless, the variance of the EOF representing the SNAO is somewhat lower than the variance of the standard run. This means that the SNAO will not occur more often when the SST pattern in the Atlantic Ocean is changed.

The location and strength of the SNAO changed significantly with the changed SST pattern. This can clearly be seen in Figure 4.8b. In this figure the difference between the EOF3 of the hfx10 run and EOF2 of the standard run (Figure 3.2b) is presented. From this figure it appears that the SNAO of the hfx10 case is shifted to the north-east. For the hfx10 run, the EOF pattern is 1 hPa higher in the east, while it is decreased by 2.5 hPa over the mid-Atlantic Ocean. This lowering is caused by southward movement of the negative pole over Greenland and the eastward shift of the positive pole.

Another way to investigate the difference between the SNAO of the standard run and the SNAO of the hfx10 run is to construct a histogram of the SLP anomalies over the domain [7.5°W-30°E, 40°N-70°]. This area is chosen, because this area is over Europe and it is interesting to know how the SLP anomalies will change over Europe. The histogram shows how often a certain sea level pressure anomaly over the domain occurred. The results are presented in Figure 4.9a.

It appears that in the hfx10 run the anomalies occurred almost equally to the standard run. However, a small increase in extreme negative SLP anomalies occurred in the hfx10 run. This is visible because more outliers are visible. However, this increase is very small.

4.5.2 SNAO structure of hfx-10 run

To identify which EOF mode belongs to the SNAO of the hfx-10 run is more difficult. The reason for that is that both the second and the third EOF of the hfx-10 mode look quite the same as SNAO EOF mode of the standard (Figure 3.2b). This can be seen in Figure 4.10, where the second and the third

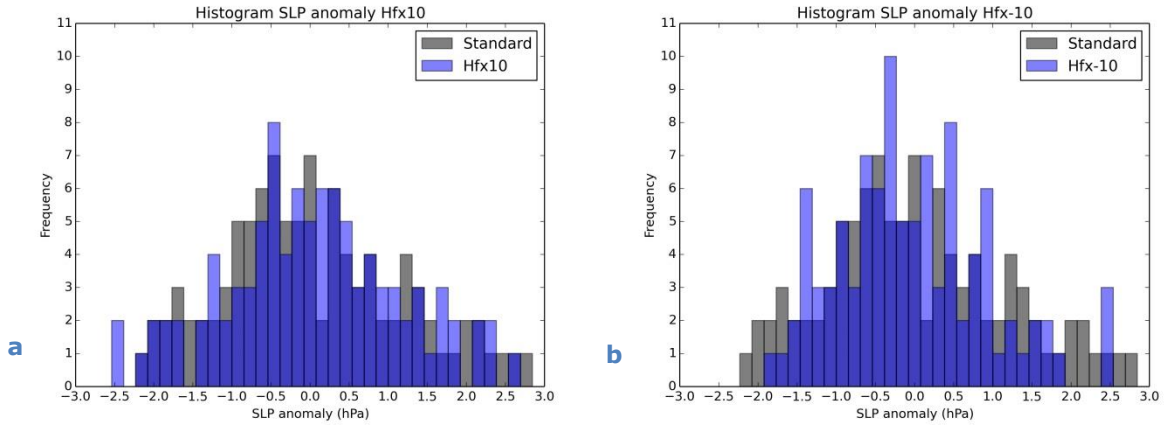

Figure 4.9: a) Histogram of the hfx10 run (blue) and the standard run (black) sea level pressure anomaly over the domain of [7.5°W-30°E, 40°N-70°N]. b) The same as Figure 4.9a, but for the hfx-10 run.

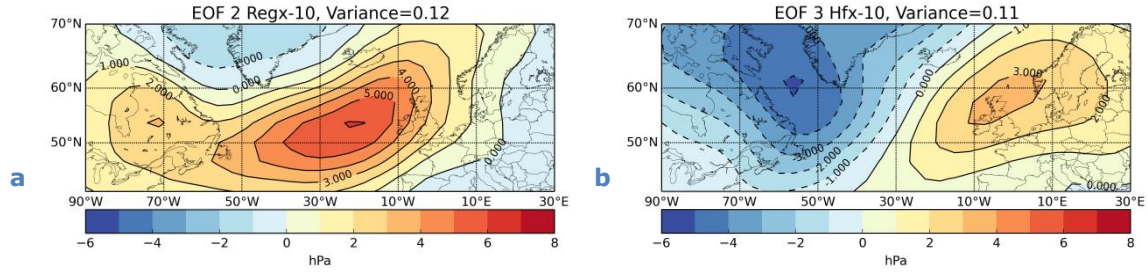

Figure 4.10: EOF2 (a) and EOF3 (b) of the hfx-10 run.

EOF mode is presented. For the sake of completeness, the main for EOF modes belonging to the hfx-10 run are presented in Appendix 1. The positive center of the second EOF mode is shifted to the west and the negative pole over Greenland is not present anymore. To the opposite of that, the negative pole of the third EOF mode is stronger than the standard run and the positive pole is weaker and shifted more to the east. Both EOF modes have the SW-NE orientation, which indicates a SNAO (Bladé et al., 2012a).

In Figure 4.9b the histogram of the sea level pressure anomalies of the hfx-10 run and the standard run over the domain of [7.5°W-30°E, 40°N-70°] is present. It can be seen that the outliers in the histogram mainly belong to the standard run. This means that less extreme sea level pressure anomalies occurred during the hfx-10 run than in the standard run.

4.6 Ensemble runs

The setup of the ensemble experiment is completely different than the setup of the 100-year run, because of that these two experiments are treated separately. Due to the fact that only a clear response of the heat fluxes multiplied by 10 was visible in the 100-year runs, only the results of the hfx10 and hfx-10 runs of the ensemble runs will be presented.

In Figure 4.11 the temperature difference between the hfx10/hfx-10 ensemble runs is presented.

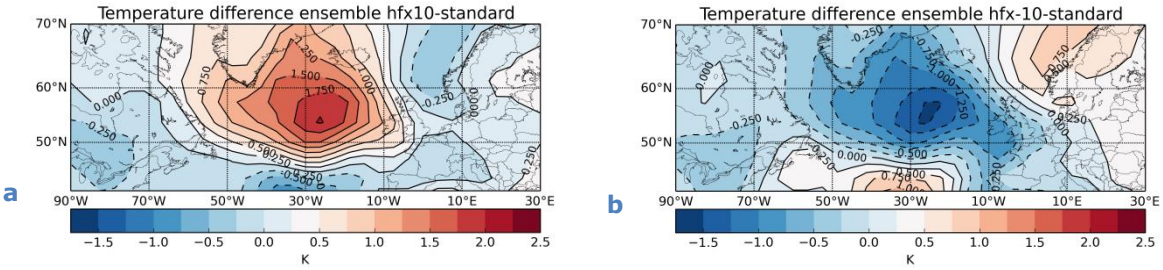

Figure 4.11: Same as Figure 4.3a and Figure 4.4b, but now for the ensemble runs.

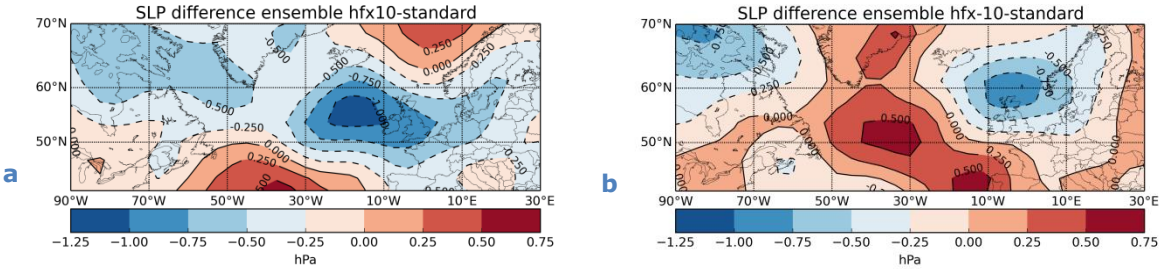

4.12: Same as Figure 4.7a and Figure 4.7b, but for the ensemble runs.

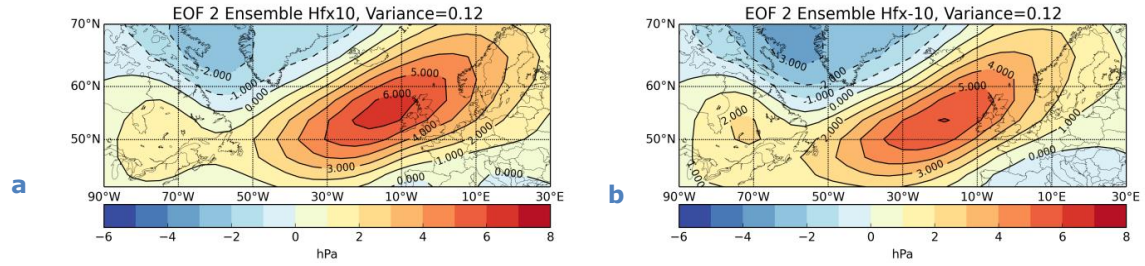

Figure 4.13: The EOF mode that resembles the SNAO for the hfx10 ensemble run (a) and the hfx-10 ensemble run (b).

Again for the hfx10 run, a positive difference occurred over the mid-Atlantic Ocean and a negative difference to the west of Norway and around 40°N,30°W. This is the same pattern as occurred in the 100-year run. However, the magnitude is much smaller for the ensemble runs compared to the 100-year runs. Also for the hfx-10 ensemble run the same pattern occurred as the hfx-10 of the 100-year run, negative difference over the mid-Atlantic ocean and slightly positive differences to the west of Norway and around 40°N,30°W.

The patterns of the SLP difference of the hfx10/hfx-10 ensemble are also comparable to the SLP differences of the hfx10/hfx-10 100-year runs. In Figure 4.12 the differences between the JA average SLP of the hfx10/hfx-10 ensemble runs and the standard run are presented. Although the difference of the ensemble runs are much smaller, like the temperature differences.

For the ensemble runs, the same analysis methods are used as for the hfx10 100-year run, namely the EOF analysis and the histogram. The EOF modes of the hfx10 and hfx-10 ensemble run that resemble the SNAO are presented in Figure 4.13. Again, this is the second EOF mode, and the explained variance is equal to the explained variance of the standard run, 12%. For the sake of completeness, the EOF modes of the hfx-10 and hfx10 ensemble runs are presented in Appendix 2.

As can be seen in Figure 4.13 and Figure 3.2b, a clear difference exists between the standard SNAO EOF mode and the hfx10 and hfx-10 SNAO EOF modes. The strength of the negative pole of the EOF of the SNAO in the hfx10 ensemble runs is much weaker than the negative pole in the standard run. This difference is around 1-2 hPa. This is due to the fact that the negative pole is shifted to the north.

In the hfx-10 of the ensemble run the SNAO structure is still visible (Figure 4.13b), contrary to the hfx-10 100-year run. The strength of the hfx-10 SNAO is weakened a little. However, the location of the centres are still on the same location.

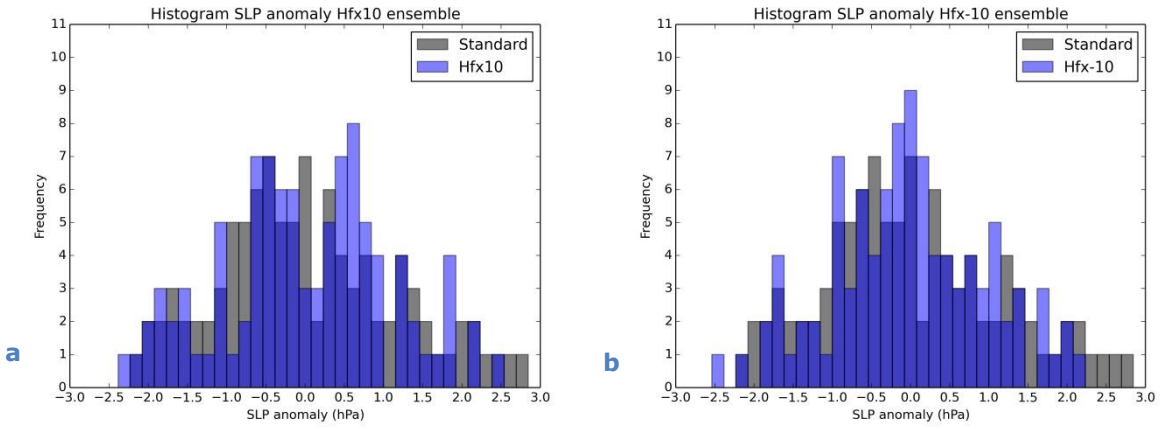

Figure 4.14 Same as Figure 4.9a and Figure 4.9b, but for the hfx10 and hfx-10 ensemble runs.

From the histogram of the SLP anomalies of the hfx10 and hfx-10 of the ensemble runs (Figure 4.14a and 4.14b), it appears that less extreme outliers are present in the hfx-10 ensemble run. This is comparable to the histogram of the hfx-10 100-year run. The histogram of the hfx10 ensemble run is also equally distributed hfx10 100-year run, almost equal amount of positive extreme outliers and a few more negative extreme outliers.

The most important finding in this chapter is that the SNAO pattern shifts to the NE when the extra heat flux pattern multiplied by 10 is added to the regular heat fluxes. Also, a small increase in the amount of outliers in the sea level pressure anomalies can occur when the extra heat flux pattern is added. When the extra heat flux pattern multiplied by 10 is extracted from the regular heat fluxes, the SNAO signal weakened very much. Next to that, less extreme outliers are present in this run. This shift in pattern of the SNAO is found in both the 100-year runs and the ensemble runs.

However, the differences of the ensemble run are much smaller compared to the 100-year run. This can be explained by the duration a different SST pattern is given to the ocean. In the ensemble runs, only for 3 months the SST is adapted, while the SST is changed for 100 years in the 100-year runs. Due to this difference, the response of the ensemble runs is much weaker.

5. Discussion

In this chapter the main results that are shown in Chapter 3 and Chapter 4 will be discussed in more detail. These are results or figures from the previous chapters that need more explanation to complete the results.

5.1 Comparison SPEEDO model and reanalysis data

In section 3.2 it is mentioned that the global precipitation is overestimated by 16,4% by the SPEEDO model, compared to the reanalysis data. Precipitation is not of importance by determining the SNAO, so not a lot of attention is paid to it. However, it is a clear difference between the SPEEDO model and reanalysis data, and it is interesting to investigate what is causing this difference.

A reason for the difference between the SPEEDO model and the reanalysis data can be the coarse resolution of the model (3.75°). Severijns and Hazeleger (2010) mentioned in their paper the difference between the precipitation in the tropical region. In the African and Amazon tropical region the precipitation in the SPEEDO model is also overestimated compared to reanalysis data. In the tropical Atlantic region the precipitation is underestimated. These where typical features of coarse resolution climate models (Dai et al, 2009; Schmidt et al, 2006). Next to that, the cloud cover is also overestimated over the North Atlantic (Severijns and Hazeleger, 2010). Probably this can also cause the overestimation of the precipitation in that region.

Another remarkable difference between the SPEEDO model and the reanalysis data is the presence of the negative pole of the SNAO in the SPEEDO data, while the negative pole is not visible in the SNAO of the reanalysis data. Another difference that is less obvious, but also present, is that the positive pole is 1 hPa lower for the SNAO resembled by the SPEEDO output, compared to the SNAO resembled by the reanalysis data. These two differences are coupled.

In Figure 3.3b and 3.4b it is visible that the Azores High is overestimated by the SPEEDO model by around 5 hPa. It is also visible that in the complete domain, except over Canada, the average JA MSLP pattern is overestimated. The SNAO is characterized by an increased pressure over northwest Europe and decreased pressure over Greenland (Bladé et al., 2012a). When the SLP over the UK is overestimated, the increased pressure belonging to a SNAO is less visible, resulting in a weaker positive pole of the SNAO. The SLP is also overestimated over Greenland, causing a larger anomaly between the average SLP over Greenland and the SLP belonging to the SNAO, resulting in the negative pole over Greenland. This means that the overestimation of the SLP in the SPEEDO model causes the differences found between the SNAO of the reanalysis data and the SPEEDO model.

The differences between the SNAO pattern of the reanalysis data and SPEEDO output can also explain the differences in the correlation maps (Figure 3.5). The presence of the negative pole over Greenland in the SPEEDO model can explain the correlation between the SNAO and the precipitation over this area. Probably more precipitation will occur over Greenland during a positive phase of the SNAO. Over Greenland, the pressure will drop more extremely in the SPEEDO model than in the reanalysis data, causing the presence of the negative pole. So in the SPEEDO model, the precipitation can correlate to this negative pole. However, in the reanalysis data the precipitation over Greenland can also increase during a positive phase of the SNAO, but the SLP anomaly between the average SLP pattern and the SLP pattern belonging to a SNAO over Greenland is smaller, so this cannot be correlated due to the absence of the SLP anomaly.

The differences in correlation of temperature in SW Europe can be explained by the location of the positive pole of the SNAO. In the SPEEDO model, this pole is situated more to the south, and also partly over SW-Europe, while this is not the case for the reanalysis data. So again the temperature in

the area of SW-Europe can be correlated to the SLP anomaly in the SPEEDO model, while this SLP anomaly is absent in the reanalysis data.

5.2 The sensitivity of the SNAO on the SST

In Chapter 4 the non-linearity of the temperature increase between the areas where the heat flux is added and extracted to or from the regular heat fluxes from the atmosphere to the ocean is discussed. For example in Figure 4.2, where the time series of the temperature for the different runs (hfx10/5/2/1 and hfx-10/5/2/1) are visible. The main result of this figure is that the temperature increase of the runs multiplied by 10 is strong in the areas where the heat flux is added, but the decrease of temperature is not visible in the areas where the heat flux multiplied by 10 is extracted. The idea is that the temperature decrease is not visible, because the colder ocean causes more turbulence in the ocean, causing a deeper mixed layer. By the deepening of the ocean the lower temperature faded away.

In figure 4.2b something remarkable is visible. In this figure the temperature of the heat flux multiplied by -10/-5/-2/-1 run over the domain of [50°W-10°W] is presented. In this area, the heat flux is extracted from the regular heat fluxes. It is visible that the temperature of the hfx-10 run is in the same order as the standard run, but the temperature of the hfx-1 and the hfx-2 runs are constantly around 2 degrees lower than the standard run and the hfx-5 run is constantly around 1 degree lower than the standard run. This can be caused by the existing of a tipping point. This means that when enough heat is extracted from the ocean, the turbulence in the ocean will occur. When less heat is extracted, the influence of the extracted heat flux on the turbulence is not large enough that the turbulence will occur, causing the sea surface layer will cool. However, this effect can only be seen in the hfx-10 run over the area of [50°W-10°W], but not in the hfx10 run over the area of [10°W-30°E], where the same happened.

The spatial figures of the temperature differences (Figure 4.3a and Figure 4.3b) show that the temperature difference is smaller in the hfx-10 run over the domain of [50°W-10°W] than the temperature difference of the hfx10 run over the domain of [10°W-30°E]. This is remarkable because in the domain of [50°W-10°W] the heat flux is extracted with values up to 150 W/m^2, while the extracted heat flux in the other domain is less, 100 W/m^2. So in the area where more heat flux is extracted, the temperature decrease is less. This can only be explained by the existing of a tipping point.

The non-linearity of the temperature can also be seen in the difference in SLP pattern, Figure 4.7. The hypothesis exists that the relation between the near surface air temperature and the SLP can be explained by the development of a thermal high/low. However, this relation could not be proven in this study. The correlation between the temperature difference and SLP difference in the domain of [50°W-10°W,50°N-60°N] is only -0.17. Next to that, the calculated divergence or differences in the geopotential height over the domain of interest gave no results that indicate the development of a thermal high or thermal low. However, the non-linearity that is visible in the difference of the near-surface air temperature is also visible in the SLP difference, so probably a relation exists.

The difference in the SLP pattern caused the shift of the SNAO of the hfx10 run. In areas where the positive SLP differences are present the SNAO signal became stronger, and in the areas where the negative SLP differences are present the SNAO signal disappeared. This is clearly visible for the hfx10 run over the mid-Atlantic Ocean (Figure 4.8b).

The behaviour of the hfx-10 SNAO is special. In the hfx-10 run the SNAO characteristics of the ocean are removed, and this has an influence on the spatial structure of the SNAO. The SNAO pattern is still visible in the EOF analysis of the hfx-10 run, but it is divided over two EOF modes, EOF2 and EOF3 (Figure 4.10). This means that the SNAO pattern merged with other patterns, which are not of

importance during the summer months. This implies that the SNAO weakened very strongly or even disappeared in the hfx-10 run. The weakening of the SNAO in the hfx-10 can also be seen in the histogram of the hfx-10 run (Figure 4.9b). Less extreme SLP anomalies will occur over Europe, which were a characteristic of the SNAO.

Another interesting aspect of the histogram is that more negative extreme outliers are present in the histogram of the hfx10 than positive extreme outliers. This can be explained by the same principle as discussed in section 5.1, the overestimation of the SLP in the SPEEDO model. When the SLP is overestimated, it is easier to have strongly negative extreme anomalies of the SLP than strongly positive extreme outliers of the SLP. This has also caused that the distribution of the SLP anomalies have their peak below zero, so more often slightly negative SLP anomalies occur.

6. Conclusions and recommendations

In this study the impact of the SST on the SNAO is investigated. Probably a relation between the SST and the winter NAO exists (Cassou and Terray, 2001; Sutton and Hodson, 2003), but to the author's knowledge, this relation has never been investigated for the summer NAO. For this reason the relation is investigated by performing a sensitivity study. The sensitivity study is performed by imprinting the SST pattern belonging to the SNAO to the ocean in the Atlantic region. In this study, a model of intermediate complexity is used: the SPEEDO model (Severijns and Hazeleger, 2010).

It was the first time the SPEEDO model was used to investigate the SNAO, yet SPEEDO was able to reproduce the SNAO. The spatial pattern of the SPEEDO output was comparable to reanalysis data and to the SNAO found by Folland et al. (2009) and Bladé et al. (2012a). Also the explained variance of the SNAO of the SPEEDO output, reanalysis data and the paper of Folland et al. (2009) was roughly the same, respectively 12%, 15% and 18%.

The SST pattern belonging to the SNAO is imprinted by adding or extracting an extra heat flux pattern to or from the ocean. This extra heat flux pattern is an extra compound to the system. It is chosen to imprint the SST in this way, so that the ocean can responds on the extra heat flux pattern and by that the ocean can influence the atmosphere. This method was performed earlier by Haarsma and Hazeleger (2007).

The pattern of the extra heat flux that is added or extracted from the ocean has three important areas where the heat flux is large. However, the sign of the heat flux in these areas is not the same. In the mid-Atlantic Ocean the area with the strongest heat flux is present. To the west of Norway and around 40°N,30°W the other two important areas are present. These two areas have the opposite sign as the mid-Atlantic Ocean area. Due to this opposite sign, the SST changes in these areas also have an opposite sign.

The ocean mixed layer reacts differently on adding or extracting extra heat to or from the ocean. When heat is extracted from the ocean, the mixed layer becomes colder. When the mixed layer becomes colder, this layer becomes unstable and vertical mixing will take place. Due to this mixing, the depth of the mixed layer will grow and the lower temperature of the upper ocean disappeared. When heat is added to the ocean, the mixed layer becomes more stable, warmer and thinner. This causes the effect of warming or cooling of the ocean to be non-linear between the three areas.

In the areas where the heating or cooling of the ocean took place, the sea level pressure over these areas also changed. In the areas where the ocean became colder, the sea level pressure became higher and vice versa. So due to the changed SST pattern, the SLP pattern changed and that caused the pattern of the SNAO to change significantly. When the extra heat flux pattern is extracted from the ocean for 100 years, the SNAO pattern weakened very strongly or even disappeared. This can be explained by the fact that the SST pattern belonging to the SNAO is extracted from the ocean, so the SST pattern of the ocean is less favourable for the development of a SNAO. The SNAO pattern found in the ensemble run where the heat flux is extracted is also weakened. Although, the weakening is less strong, because the duration that the heat flux pattern is extracted in the ensemble runs is less than in the 100-year runs.

When an extra heat flux pattern belonging to the SNAO is added to the ocean for 100 years, the positive pole of the SNAO is slightly shifted to the north-east and the negative pole is slightly shifted to the south, causing a stronger negative pole over Greenland of the EOF mode. The positive pole of the EOF mode is weakened a little bit. Next to that, the probability exists that more extreme SLP anomalies in the domain of [7.5°W-30°E,40°N-70°N] will occur. However, this increase of extreme

SLP anomalies is small. The shift of the SNAO pattern of the ensemble run where the heat flux pattern is added is less obvious than the shift of the SNAO in the 100-year run. However, the positive pole is shifted to the south-west and the negative pole is shifted to the north, resulting in a less strong negative pole over Greenland. The main conclusion of this research is that from this study we conclude that a relation exists between the SNAO and the SST.

6.1 Recommendations for further research

This study is performed using a fast model of intermediate complexity. This is very suitable for an orientating study to investigate an effect. However, the resolution of the model is very coarse, causing e.g. an error in the amount of precipitation of the model. For further research, it would be interesting to investigate if the relation between the SST and the SNAO found in this study is also present in more complex models, e.g. the EC-EARTH or CMIP5 models.

As mentioned in Chapter 5, some hypothesis still exist, it was not possible to investigate these hypothesis in more depth in the scope of this research. It would be interesting to investigate the principle behind the processes. For example, it would be interesting to know if a tipping point exists in the development of the depth of the mixed layer. This can be used in future studies regarding the exchange of heat between the ocean and the atmosphere.

The SNAO has a certain impact on the weather in Europe during the high-summer months. Because of that it is interesting to know how the pattern of the SNAO will change in the future with increasing greenhouse gas concentrations. The increasing greenhouse gas concentration causes higher temperatures. The SNAO pattern might also change due to these increasing greenhouse gases. Because of that it would interesting to extend this research.

Acknowledgement

I really want to thank my two supervisors, Wilco and Leo. You both helped me a lot with discussion the results and the set-up of the study. I also learned a lot from this, and now I have more knowledge and insights in performing a research. Next to that, I want to thank two persons who also really helped me a lot, Camiel and Kees. Camiel, thank you for answering all my questions about the SPEEDO model and when you helped me when I was completely stuck. Kees, you were always there to help when I had a question about the model or about programming. Thank you for that. Last, I want to thank my fellow MAQ-MSc students who were also writing their thesis, for the in depth discussions we had, but also for the nice conversations about everything.

References

Ansell, T., Jones, P., Allan, R., Lister, D., Parker, D., Brunet, M., Moberg, A., Jacobeit, J., Brohan, P. and Rayner, N., 2006, Daily Mean Sea Level Pressure Reconstructions for the European–North Atlantic Region for the Period 1850–2003. Journal of Climate, 19.

Barnston, A.G. and Livezey, R.E., 1987, Classification, seasonality and persistence of low-frequency atmospheric circulation patterns. Monthly weather review, 115: 1083-1126.

Bladé, I., Fortuny, D., Oldenborgh, G.J. and Liebmann, B., 2012a, The summer North Atlantic Oscillation in CMIP3 models and related uncertainties in projected summer drying in Europe. Journal of Geophysical Research: Atmospheres (1984–2012), 117.

Bladé, I., Liebmann, B., Fortuny, D. and van Oldenborgh, G.J., 2012b, Observed and simulated impacts of the summer NAO in Europe: implications for projected drying in the Mediterranean region. Climate dynamics, 39: 709-727.

Cassou, C. and Terray, L., 2001, Oceanic forcing of the wintertime low-frequency atmospheric variability in the North Atlantic European sector: A study with the ARPEGE model. Journal of Climate, 14: 4266-4291.

Cornes, R.C., Jones, P.D., Briffa, K.R. and Osborn, T.J., 2013, Estimates of the North Atlantic Oscillation back to 1692 using a Paris–London westerly index. International Journal of Climatology, 33: 228-248.

Dai, A., Wigley, T., Boville, B., Kiehl, J. and Buja, L., 2001, Climates of the twentieth and twenty-first centuries simulated by the NCAR climate system model. Journal of Climate, 14: 485-519.

Feldstein, S.B., 2007, The dynamics of the North Atlantic Oscillation during the summer season. Quarterly Journal of the Royal Meteorological Society, 133: 1509-1518.

Folland, C.K., Knight, J., Linderholm, H.W., Fereday, D., Ineson, S. and Hurrell, J.W., 2009, The summer North Atlantic Oscillation: Past, present, and future. Journal of Climate, 22.

Frankignoul, C., Czaja, A. and L'Heveder, B., 1998, Air--Sea Feedback in the North Atlantic and Surface Boundary Conditions for Ocean Models. Journal of Climate, 11.

Greatbatch, R.J. and Rong, P.-p., 2006, Discrepancies between different Northern Hemisphere summer atmospheric data products. Journal of Climate, 19.

Haarsma, R.J. and Hazeleger, W., 2007, Extratropical atmospheric response to equatorial Atlantic cold tongue anomalies. Journal of Climate, 20.

Hartmann, D.L., 1994, Global physical climatology. Academic press

Hurrell, J.W., 1995, Decadal trends in the North Atlantic oscillation. Science, 269: 676-679.

Hurrell, J.W. and Deser, C., 2010, North Atlantic climate variability: the role of the North Atlantic Oscillation. Journal of Marine Systems, 79: 231-244.

Kalnay, E., Kanamitsu, M., Kistler, R., Collins, W., Deaven, D., Gandin, L., Iredell, M., Saha, S., White, G. and Woollen, J., 1996, The NCEP/NCAR 40-year reanalysis project. Bulletin of the American meteorological Society, 77: 437-471.

Kushnir, Y., Robinson, W., Bladé, I., Hall, N., Peng, S. and Sutton, R., 2002, Atmospheric GCM response to extratropical SST anomalies: Synthesis and evaluation. Journal of Climate, 15.

Linderholm, H.W., Folland, C.K. and Jeong, J.-H., 2012, C20C project on the summer North Atlantic Oscillation.

Portis, D.H., Walsh, J.E., El Hamly, M. and Lamb, P.J., 2001, Seasonality of the North Atlantic Oscillation. Journal of Climate, 14.

Robertson, A.W., Mechoso, C.R. and Kim, Y.-J., 2000, The influence of Atlantic sea surface temperature anomalies on the North Atlantic Oscillation. Journal of Climate, 13.

Schmidt, G.A., Ruedy, R., Hansen, J.E., Aleinov, I., Bell, N., Bauer, M., Bauer, S., Cairns, B., Canuto, V. and Cheng, Y., 2006, Present-day atmospheric simulations using GISS ModelE: Comparison to in situ, satellite, and reanalysis data. Journal of Climate, 19: 153-192.

Severijns, C. and Hazeleger, W., 2010, The efficient global primitive equation climate model SPEEDO V2. 0. Geosci Model Dev, 3: 105-122.

Spall, M.A., Weller, R.A. and Furey, P.W., 2000, Modeling the three-dimensional upper ocean heat budget and subduction rate during the Subduction Experiment. Journal of Geophysical Research: Oceans (1978–2012), 105: 26151-26166.

Sutton, R. and Hodson, D., 2003, Influence of the Ocean on North Atlantic Climate Variability 1871–1999. Journal of Climate, 16.

Sutton, R.T., Norton, W.A. and Jewson, S.P., 2000, The North Atlantic Oscillation—What Role for the Ocean? Atmospheric Science Letters, 1: 89-100.

Vallis, G.K., 2006, Atmospheric and oceanic fluid dynamics: fundamentals and large-scale circulation. Cambridge University Press

Venzke, S., Allen, M., Sutton, R. and Rowell, D., 1999, The atmospheric response over the North Atlantic to decadal changes in sea surface temperature. Journal of Climate, 12.

Wallace, J.M. and Hobbs, P.V., 2006, Atmospheric science: an introductory survey. Academic press

Appendix 1

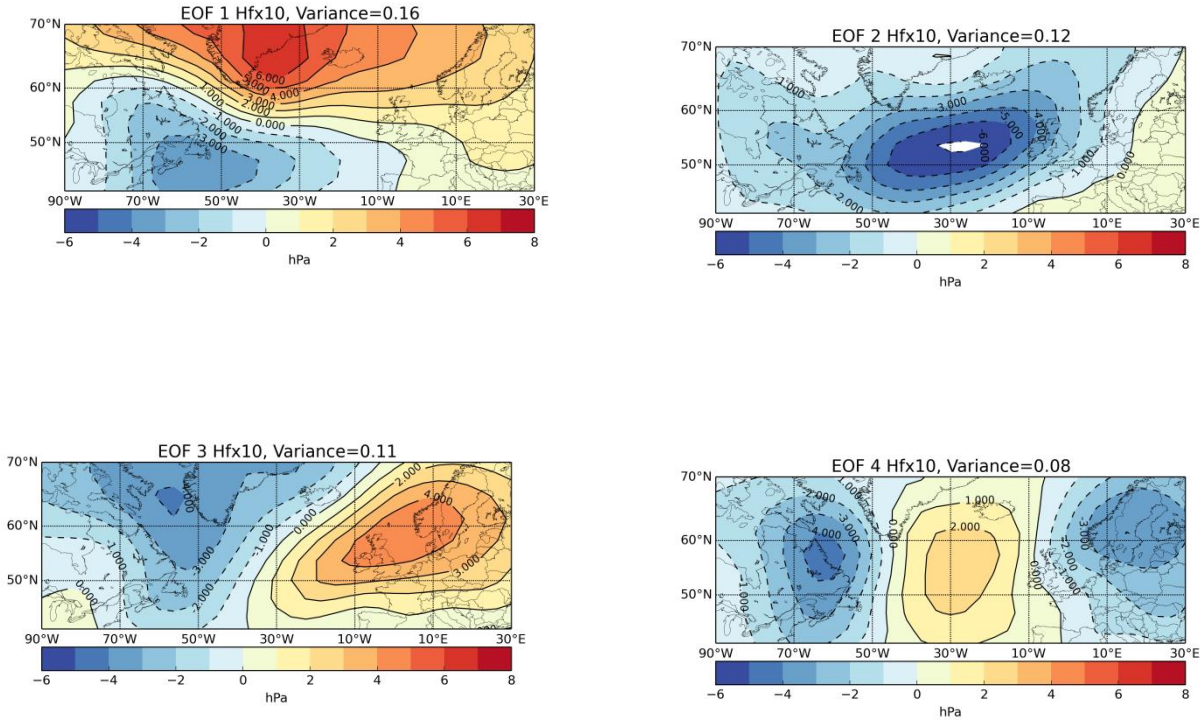

Figure App1.1: The main 4 EOF modes belonging to the hfx10 100-year run.

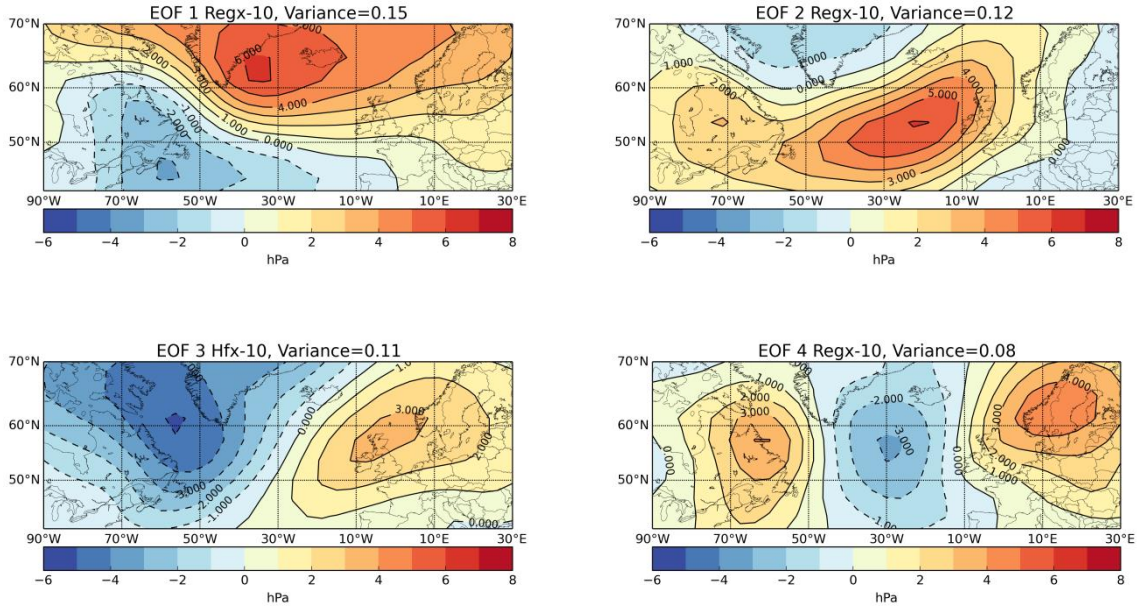

Figure App1.2: The main four EOF modes belonging to the hfx-10 100-year run.

Appendix 2

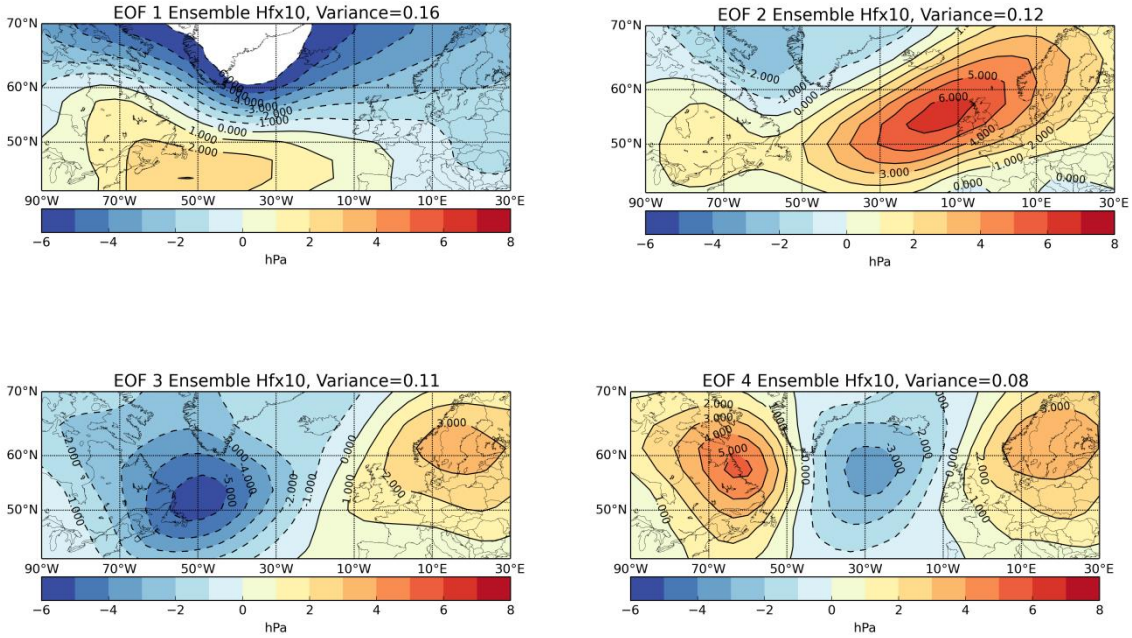

Figure App2.1: The main 4 EOF modes belonging to the hfx10 ensemble run.

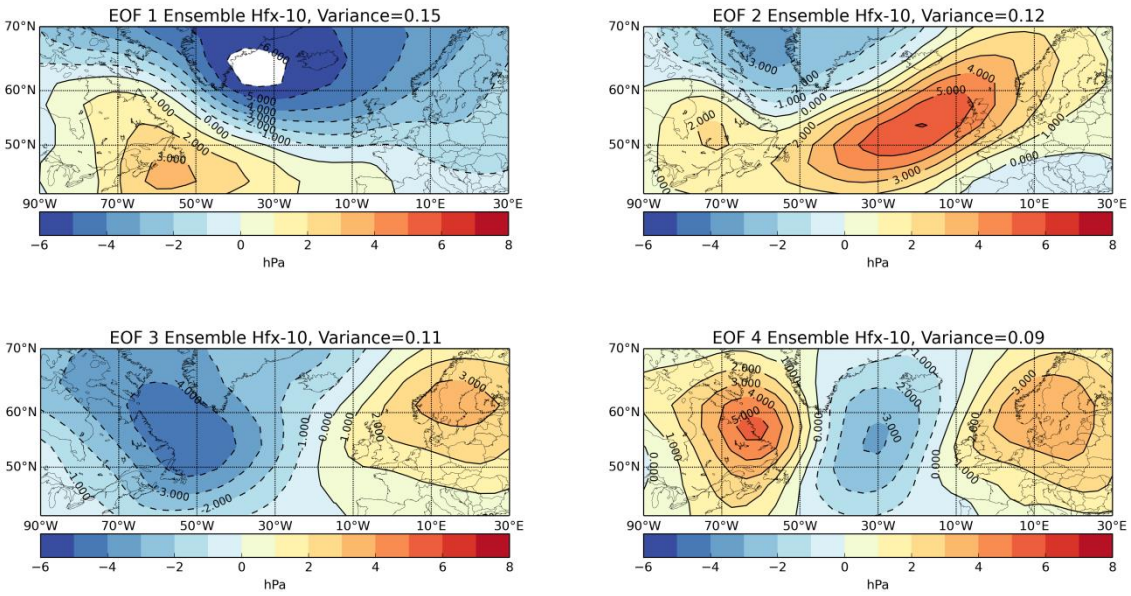

Figure App2.2: The main 4 EOF modes belonging to the hfx-10 ensemble run.